A brief history of gravitational-wave research and the gravitational-wave spectrum

Wei-Tou Ni

National Tsing Hua University

Refs: (i) WTN, GW classification, space GW detection sensitivities and AMIGO arXiv:1709.05659 [gr-qc] July 4, 2017 Plenary talk at ICGAC-IK15

(ii) S. Kuroyanagi, L-W Luo and WTN, GW sensitivities over all frequency band

(iii) K Kuroda, WTN and W-P Pan, GWs: Classification, methods of detection, sensitivities, and sources, IJMPD 24 (2015) 1530031

(iv) C-M Chen, J Nester and WTN, A brief history of GW research, Chin. J. P. (2017)

(v) WTN, GW detection in space IJMPD 25 (2016) 1530002

Outline

- Earth History
- Interferometric Detection of GW
- Discovery, Black hole distribution and Multi-Messenger Astronomy
- GW spectrum and detection sensitivities
- Cosmic Band, Quaser Astrometry Band and PTA band
- Space GW detection, new LISA and Super-ASTROD and AMIGO, Middle-Frequency Band
- Outlook

Observation-Tech Gap 100 years ago

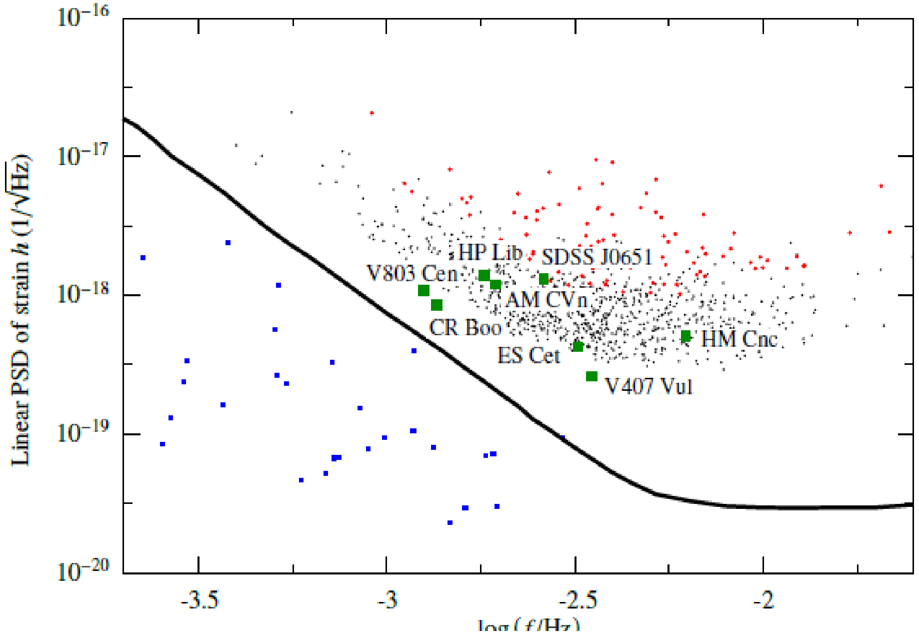

- 1916, 1918 Einstein predicted GW and derived the quadrupole radiation formula
- White dwarf discovered in 1910 with its density soon estimated; GWs from white dwarf binaries in our Galaxy form a stochastic GW background (confusion limit for space GW detection: strain, 10^(-20) in 0.1-1mHz band). [Periods: 5.4 minutes (HM Cancri) to hours](3 mHz)
- One hundred year ago, the sensitivity of astrometric observation through the atmosphere around this band is about 1 arcsec. This means the strain sensitivity to GW detection is about 10^{-5}; 15 orders away from the required sensitivity.
- Observation-Tech Gap 100 years ago: 15 orders away

Gravitational Waves – Ripples in Spacetime

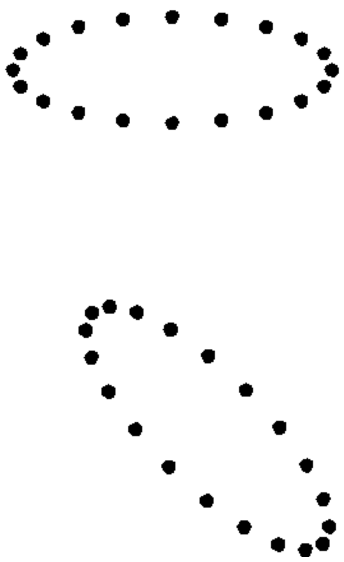

$$[\epsilon^{(1)}]_{ij} = \begin{pmatrix} 0 & 0 & 0 \\ 0 & 0 & 0 \\ 0 & 0 & 1 \end{pmatrix} \qquad [\epsilon^{(2)}]_{ij} = \begin{pmatrix} 0 & 0 & 1 \\ 0 & 0 & 0 \\ 1 & 0 & 0 \end{pmatrix}$$

$$[\epsilon^{(3)}]_{ij} = \begin{pmatrix} 0 & 0 & 0 \\ 0 & 0 & 1 \\ 0 & 1 & 0 \end{pmatrix} \qquad [\epsilon^{(4)}]_{ij} \underset{\text{GR}}{=} \begin{pmatrix} 1 & 0 & 0 \\ 0 & -1 & 0 \\ 0 & 0 & 0 \end{pmatrix}$$

$$[\epsilon^{(5)}]_{ij} \overset{\text{GR}}{=} \begin{pmatrix} 0 & 1 & 0 \\ 1 & 0 & 0 \\ 0 & 0 & 0 \end{pmatrix} \qquad [\epsilon^{(6)}]_{ij} = \begin{pmatrix} 1 & 0 & 0 \\ 0 & 1 & 0 \\ 0 & 0 & 0 \end{pmatrix}.$$

GW propagation direction: z

- Monochromatic

  A single frequency plane GW

- Wave form in time t,

  Spectral form in frequency f

- Noise power amplitude

$<n^2(t)> = \int_0^\infty (df)\, S_n(f),\ h_n(f) \equiv [f\, S_n(f)]^{1/2}$

- Characteristic amplitude

$$G_{\mu\nu} = \kappa\, T_{\mu\nu},\ R_{\mu\nu} = 8\pi G_N\, [T_{\mu\nu} - (1/2)(g_{\mu\nu} T)]$$

$A_{\mu,\beta}{}^{\beta} = 4\pi J_\mu,$

$$h_{\mu\nu,\beta}{}^{\beta} = -16\pi G_N [T_{\mu\nu} - (1/2)(\eta_{\mu\nu} T)] + O(h^2)$$

with gauge condition

$A_{\alpha,}{}^{\alpha} = 0.$

$$h_{\mu\nu} = -[(4G_N)/(c^4)] \int \{[T_{\mu\nu} - (1/2)\, g_{\mu\nu} T]/r\}_{\text{retarded}}\, (d^3x') + O(h^2)$$

In harmonic gauge

The retarded solution of equation (12) is

$A_\mu = \int (J_\mu/r)_{\text{retarded}}\, (d^3x').$

plane GW $h_{\mu\nu}(n_x x + n_y y + n_z z - ct) = h_{\mu\nu}(U)$

$$h_{\mu\nu}(u, t) \equiv h_{\mu\nu}(U) = \int_{-\infty}^{\infty} {}^{(f)}h_{\mu\nu}(f) \exp(2\pi i f U/c)\, (df) = \int_0^\infty 2f\, |{}^{(f)}h_{\mu\nu}(f)| \cos(2\pi f U/c)\, d(\ln f)$$

$$h_{\mu\nu}(U) = \int_0^\infty 2|{}^{(f)}h_{\mu\nu}(f)| \cos(2\pi f U/c)\, (df)$$
$$= \int_0^\infty 2f\, |{}^{(f)}h_{\mu\nu}(f)| \cos(2\pi f U/c)\, d(\ln f).$$

$$h_{\mu\nu}(x, y, z, t) = (c/2\pi)^3 \int {}^{(k)}h_{\mu\nu}(k_x, k_y, k_z) \exp(ik_x x + ik_y y + ik_z z - 2\pi i f t)\, (dk_x dk_y dk_z)$$

$h_c(f) \equiv 2f\, [(|{}^{(f)}h_+(f)|^2 + |{}^{(f)}h_\times(f)|^2)]^{1/2};\ h_{cA}(f) \equiv 2f\, |{}^{(f)}h_A(f)|$

Gap largely bridged

92 days
1440 orbits
83.60 kg mass

- First artificial satellite Sputnik launched in 1957.
- First GW space mission proposed in public in 1981 by Faller & Bender
- LISA proposed as a joint ESA-NASA mission; LISA Pathfinder successfully performed.
- The drag-free tech is fully demonstrated paving the road for GW space missions.

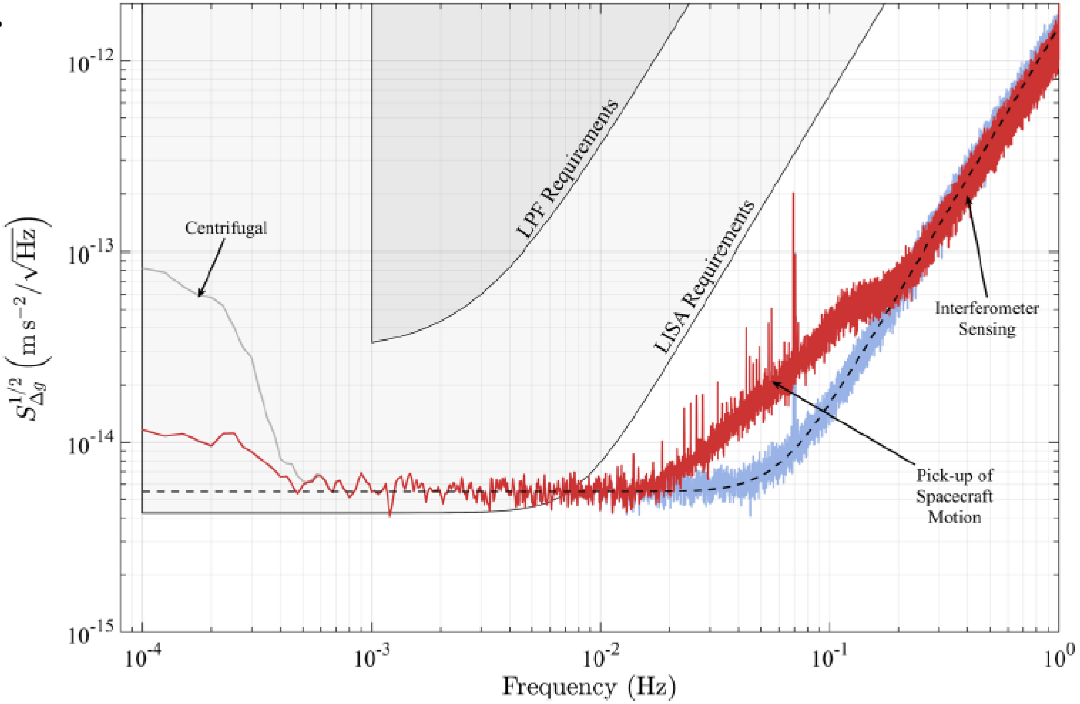

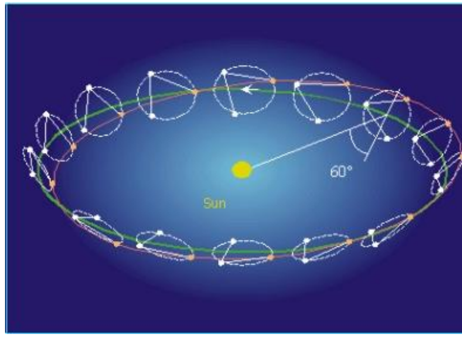

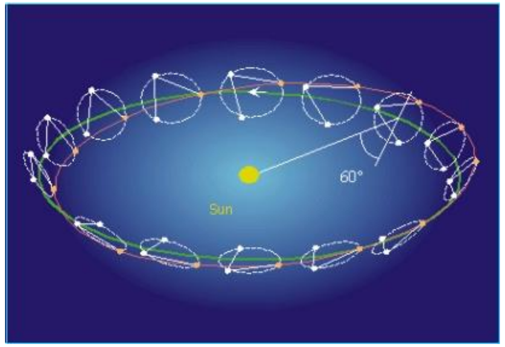

空间引力波探测
A Compilation of GW Mission Proposals LISA Pathfinder Launched on December 3, 2015

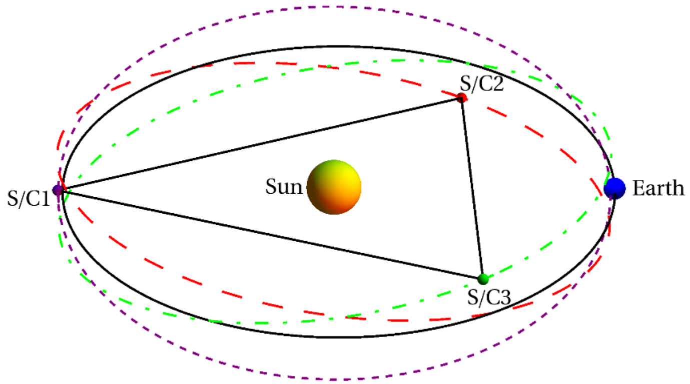

Mission Concept	S/C Configuration	Arm length	Orbit Period	S/C #
Solar-Orbit GW Mission Proposals				
LISA[65]	Earth-like solar orbits with 20° lag	5 Gm	1 year	3
eLISA[64]	Earth-like solar orbits with 10° lag	1 Gm	1 year	3
ASTROD-GW[68]	Near Sun-Earth L3, L4, L5 points	260 Gm	1 year	3
Big Bang Observer[73]	Earth-like solar orbits	0.05 Gm	1 year	12
DECIGO[72]	Earth-like solar orbits	0.001 Gm	1 year	12
ALIA[74]	Earth-like solar orbits	0.5 Gm	1 year	3
ALIA-descope[75]太极	Earth-like solar orbits	3 Gm	1 year	3
Super-ASTROD[71]	Near Sun-Jupiter L3, L4, L5 points (3 S/C), Jupiter-like solar orbit(s)(1-2 S/C)	1300 Gm	11 year	4 or 5
Earth-Orbit GW Mission Proposals				
OMEGA[81]	0.6 Gm height orbit	1 Gm	53.2 days	6
gLISA/GEOGRAWI[76-78]	Geostationary orbit	0.073 Gm	24 hours	3
GADFLI[79]	Geostationary orbit	0.073 Gm	24 hours	3
TIANQIN[82] 天琴	0.057 Gm height orbit	0.11 Gm	44 hours	3
ASTROD-EM[69,70]	Near Earth-Moon L3, L4, L5 points	0.66 Gm	27.3 days	3
LAGRANGE[80]	Near Earth-Moon L3, L4, L5 points	0.66 Gm	27.3 days	3

The observation and technology gap 100 years ago in the 10 Hz – 1 kHz band

- In the LIGO discovery of 2 GW events and 1 probable GW candidate, the maximum peak strain intensity is 10^{-21}; the frequency range is 30-450 Hz.
- Strain gauge in this frequency region could reach 10^{-5} with a fast recorder about 100 years ago;
- thus, the technology gap would be 16 orders of magnitudes.
- Michelson interferometer for Michelson-Morley experiment[10] has a strain ($\Delta l/l$) sensitivity of 5×10^{-10} with 0.01 fringe detectability and 11 m path length;
- however, the appropriate test mass suspension system with fast (30-450 Hz in the high-frequency GW band) white-light observing system is lacking.

Weber Bar (50 Years ago)
10 orders of gap abridged

- OBSERVATION OF THE THERMAL FLUCTUATIONNS OF A GRAVITATIONAL-WAVE DETECTOR* J. Weber

  PRL 1966 (Received 3 October 1966)

  Strains as small as a few parts in 10^{16} are observable for a compressional mode of a large cylinder.

- GRAVITATIONAL RADIATION* J. Weber

  PRL 1967 (Received 8 February 1967)

- The results of two years of operation of a 1660-cps gravitational-wave detector are reviewed. The possibility that some gravitational signals may have been observed cannot completely be ruled out. New gravimeter-noise data enable us to place low limits on gravitational radiation in the vicinity of the earth's normal modes near one cycle per hour, implying an energy-density limit over a given detection mode smaller than that needed to provide a closed universe.

Sinsky's Calibration in Weber's Lab

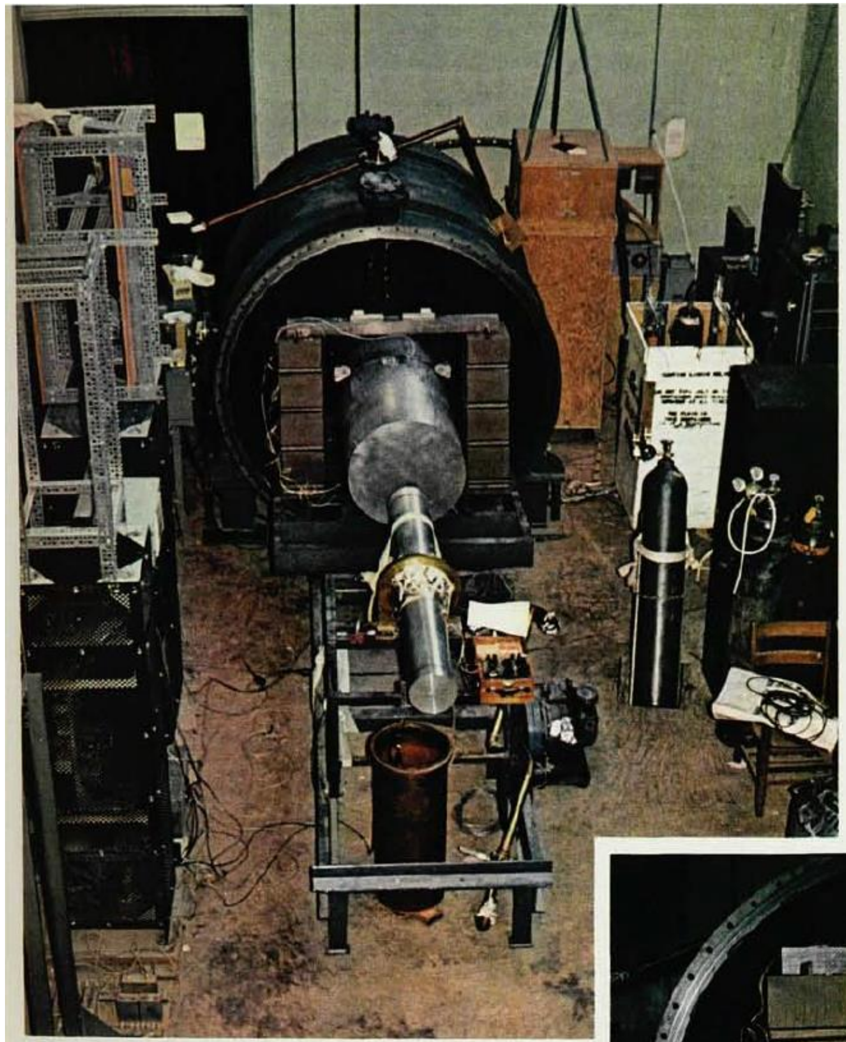

ALUMINUM CYLINDER of 1400-kg mass is suspended by a wire on acoustic filters. Piezoelectric transducers are bonded to the top surface, as shown in the closeup.

DETECTOR and dynamic gravitational field generator are shown removed from their common vacuum chamber.

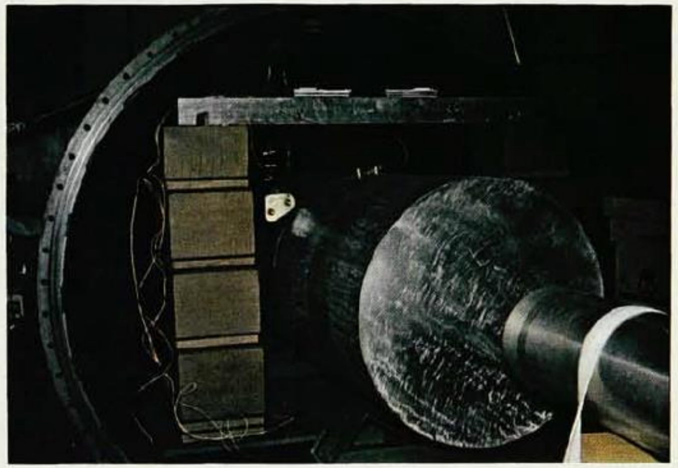

The start of precision laser interferometry for GW detection

(left) Interferometer system noise measurement at 5 kHz of Moss, Miller and Forward (1971); (right) Schematic of Malibu Laser Interferometer GW Antenna of Forward (1978)

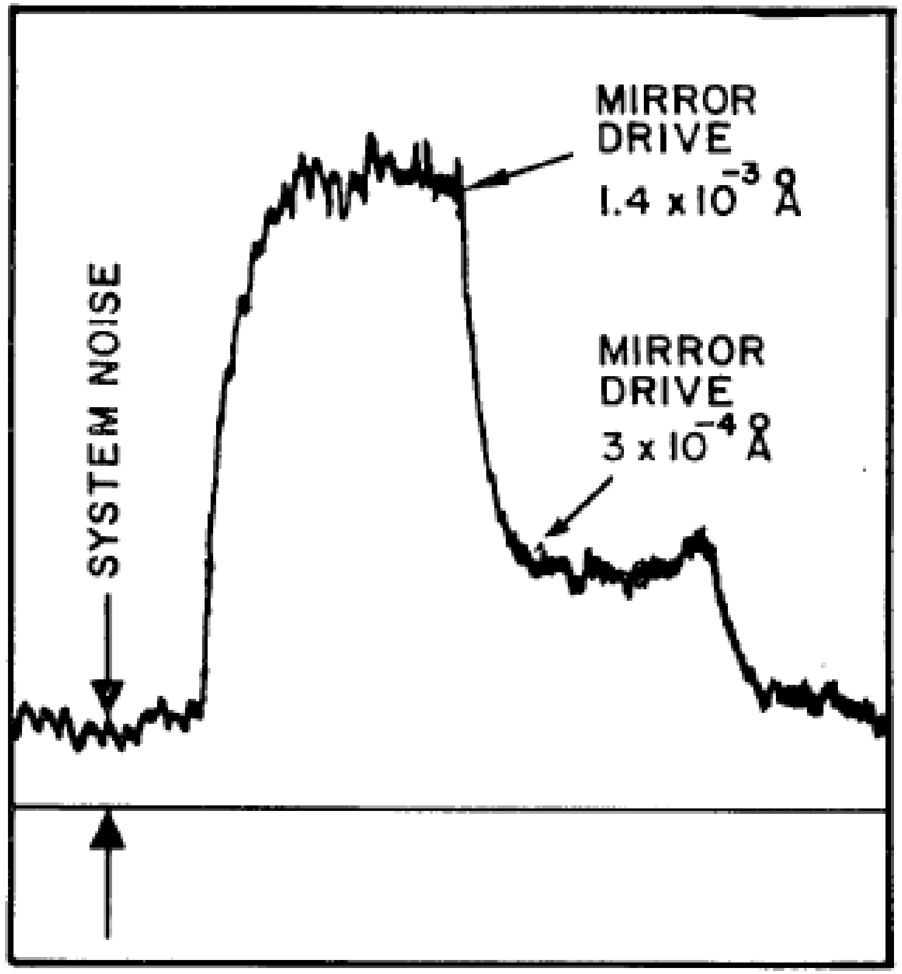

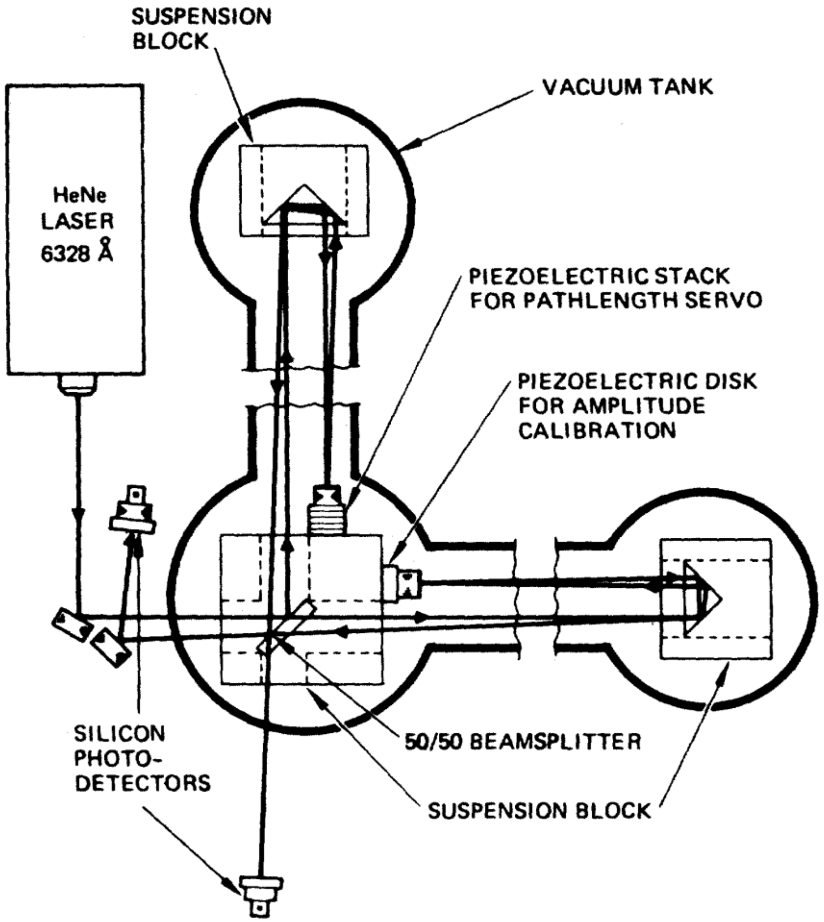

The fundamental noise sources of Weiss 1972

- km-sized interferometer proposed

- a. Amplitude noise in the laser output power;
- b. Laser phase noise or frequency instability;
- c. Mechanical thermal noise in the antenna;
- d. Radiation-pressure noise from laser light;
- e. Seismic noise;
- f. Thermal-gradient noise;
- g. Cosmic-ray noise;
- h. Gravitational-gradient noise;
- i. Electric field and magnetic field noise.

探测引力波的原型光学干涉仪盛行时期
Flourish of Prototype Optical Interferometers for GW Detection

- Hughes Research Lab (HRL) 0.75 m
- MIT prototype interferometer 1.5 m
- Glasgow prototype interferometer 10 m
- Garching prototype interferometer 30 m
- Tokyo prototype interferometer 3 m
- Paris prototype interferometer 7 m
- ISAS prototype interferometer 10 m
- NAOJ prototype interferometer 20 m
- ISAS prototype interferometer 100 m

TAMA 300 m

GEO 600 m

Laser interferometers with independently suspended mirrors. In third column, in the parenthesis either the number N of paths is given or Fabry-Perot Finesse F is given.

Interferometer	Arm length [m]	Effective optical path length [km]	Year Construction Started
Hughes Research Lab (HRL) [87,137,142]	2	0.0085 (N = 4)	1966
MIT prototype [202]	1.5	0.075 (N = 50)	1971
Garching 3 m prototype	3	0.012 (N = 4)	1975
Glasgow 1 m prototype [210]	1	0.036 (N = 36; in static test reached N = 280)	1976
Glasgow 10 m prototype [210]	10	25.5 (F-P: F = 4000)	1980
Caltech 40 m prototype	40	75	1980
Garching 30 m prototype	30	2.7 (N = 90)	1983
ISAS Tenko 10 m prototype [112]	10	1 (N= 100)	1986
U. Tokyo prototype [14,111]	3	0.42 (F-P: F = 220)	1987
ISAS Tenko 100 m prototype [114,139–141]	100	10 (N = 100)	1991
NAOJ 20 m prototype [16]	20	4.5 (F-P: F = 350)	1991
Q&A 3.5 m prototype [55]	3.5	67 (F-P: F = 30000)	1993
TAMA 300 m [184]	300	96 (F-P: F = 500)	1995
GEO 600 m [91,209]	600	1.2 (N = 2)	1995
LIGO Hanford (2 km) [1,124]	2000	143 (F-P: F = 112)	1994
LIGO Hanford (4 km) [124,130]	4000	1150 (F-P: F = 450)	1994
LIGO Livingston (4 km) [124,130]	4000	1150 (F-P: F = 450)	1995
VIRGO [5,191]	3000	850 (F-P: F = 440)	1996
AIGO prototype [205,206]	80	760/66 (F-P: east arm F= 15000; south arm F = 1300)	1997
LISM [168]	20	320 (F-P: F = 25000)	1999
CLIO 100 m cryogenic [7]	100	190 (F-P: F = 3000)	2000
Q&A 7 m [134]	7	450 (F-P: F = 100000)	2008
LCGT/KAGRA [21,109]	3000	2850 (F-P: F = 1500)	2010
Q&A 9 m [208]	9	570 (F-P: F = 100000)	2016
LIGO India [102]	4000	1150 (F-P: F = 450)	2016
ET [99]	10000	3200 (F-P: F~ 500)	Proposal under study

重力波雷射干涉探测器
基本原理

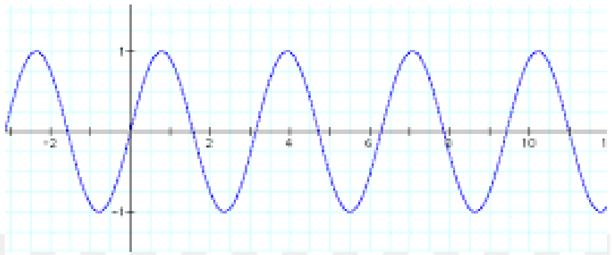

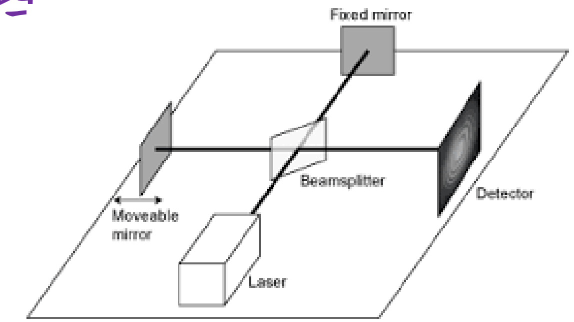

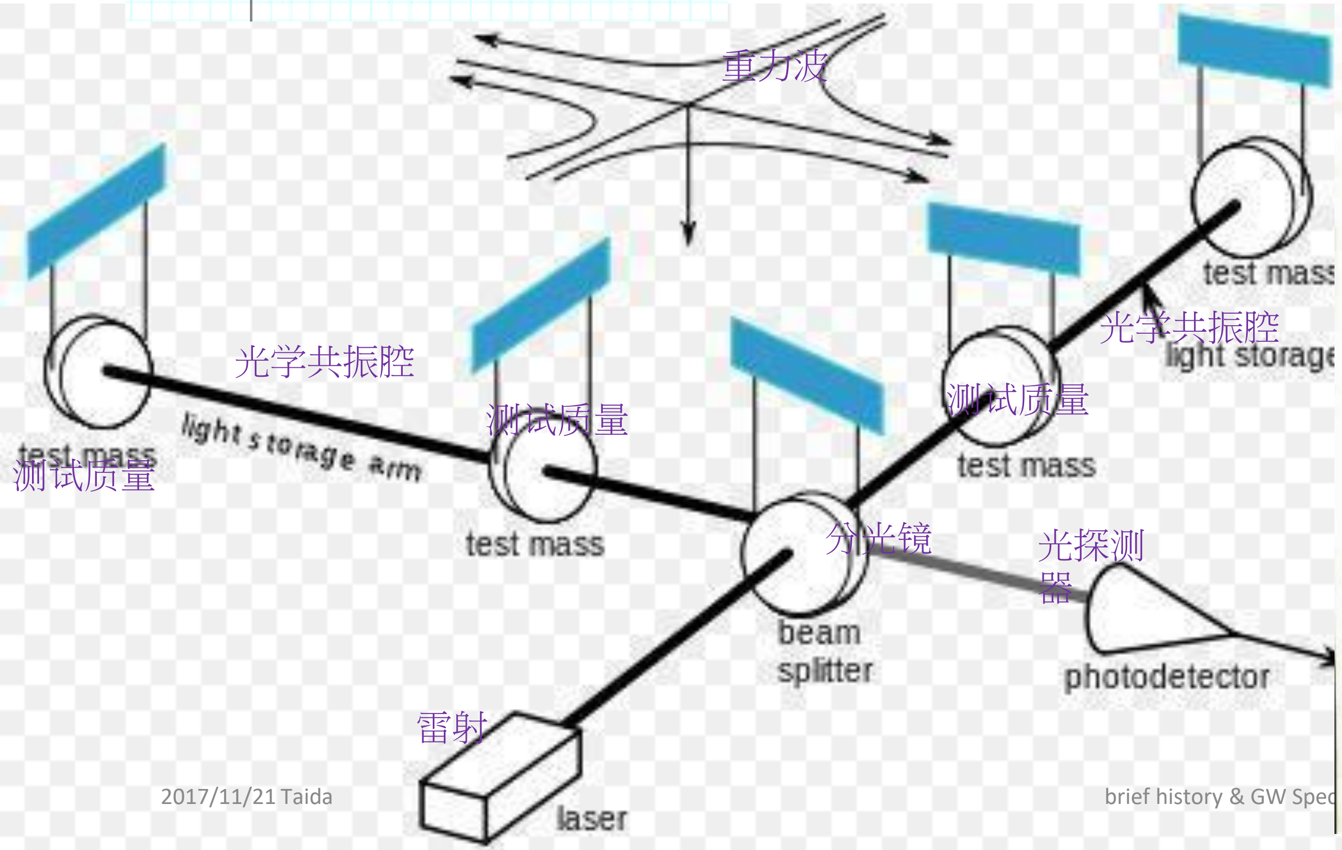

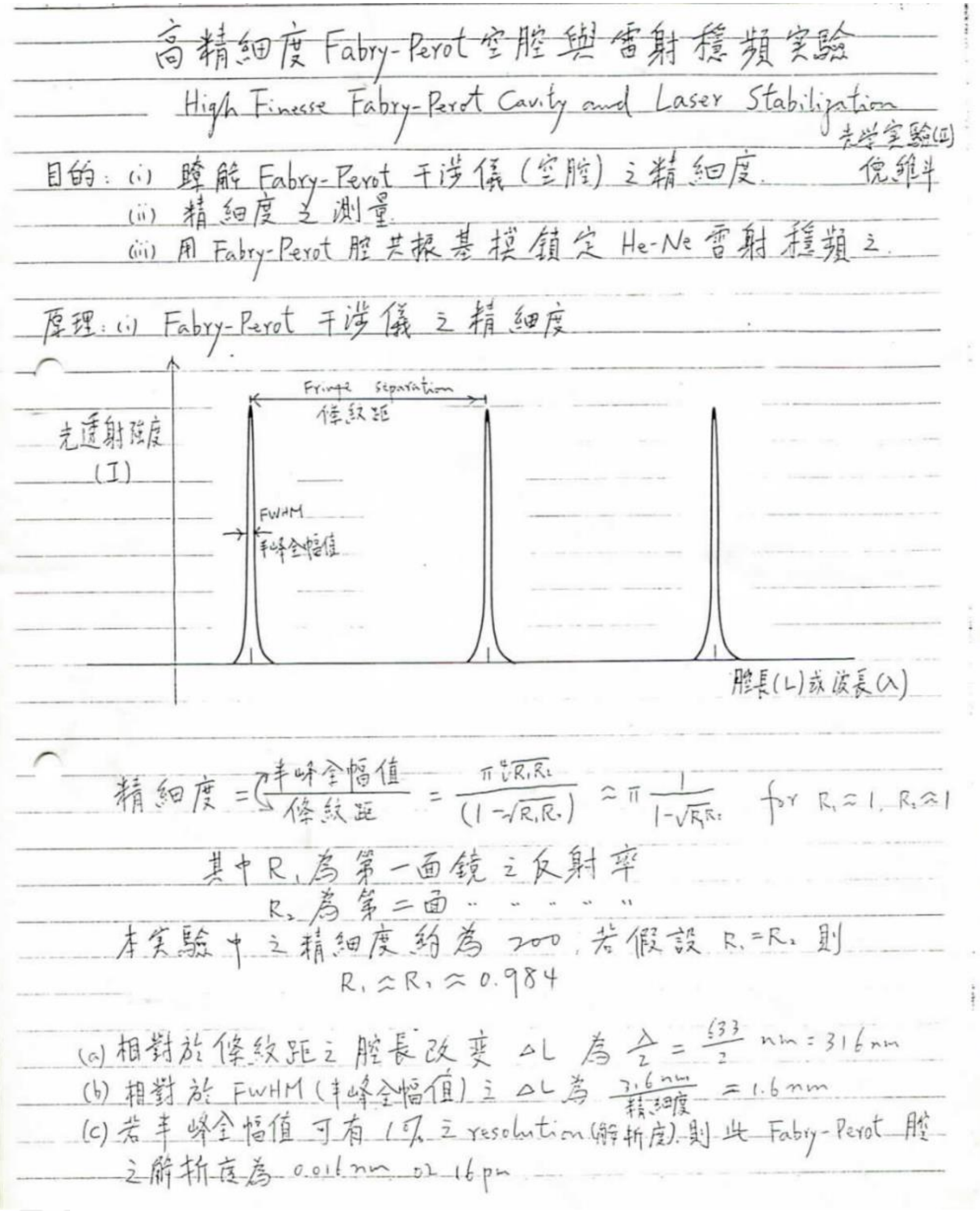

高精細度 Fabry-Perot 空腔與雷射穩頻实驗

High Finesse Fabry-Perot Cavity and Laser Stabilization

光学实驗(四)

倪維斗

目的：(i) 瞭解 Fabry-Perot 干涉儀（空腔）之精細度.

(ii) 精細度之測量.

(iii) 用 Fabry-Perot 腔共振基模鎖定 He-Ne 雷射穩頻之.

原理：(i) Fabry-Perot 干涉儀之精細度

$$\text{精細度} = \frac{\text{半峰全幅值}}{\text{條紋距}} = \frac{\pi\sqrt[4]{R_1R_2}}{(1-\sqrt{R_1R_2})} \simeq \pi\frac{1}{1-\sqrt{R_1R_2}} \quad \text{for } R_1\simeq 1,\ R_2\simeq 1$$

其中 R_1 為第一面鏡之反射率

R_2 為第二面 " " " "

本实驗中之精細度約為 200，若假設 $R_1=R_2$ 則

$R_1 \simeq R_2 \simeq 0.984$

(a) 相對於條紋距之腔長改变 ΔL 為 $\frac{\lambda}{2} = \frac{633}{2}\ nm = 316\ nm$

(b) 相對於 FWHM（半峰全幅值）之 ΔL 為 $\frac{3.6\ nm}{\text{精細度}} = 1.6\ nm$

(c) 若半峰全幅值可有 1% 之 resolution（解析度），則此 Fabry-Perot 腔之解析度為 0.016 nm or 16 pm

Interferometry for GW detection: e.g. KAGRA

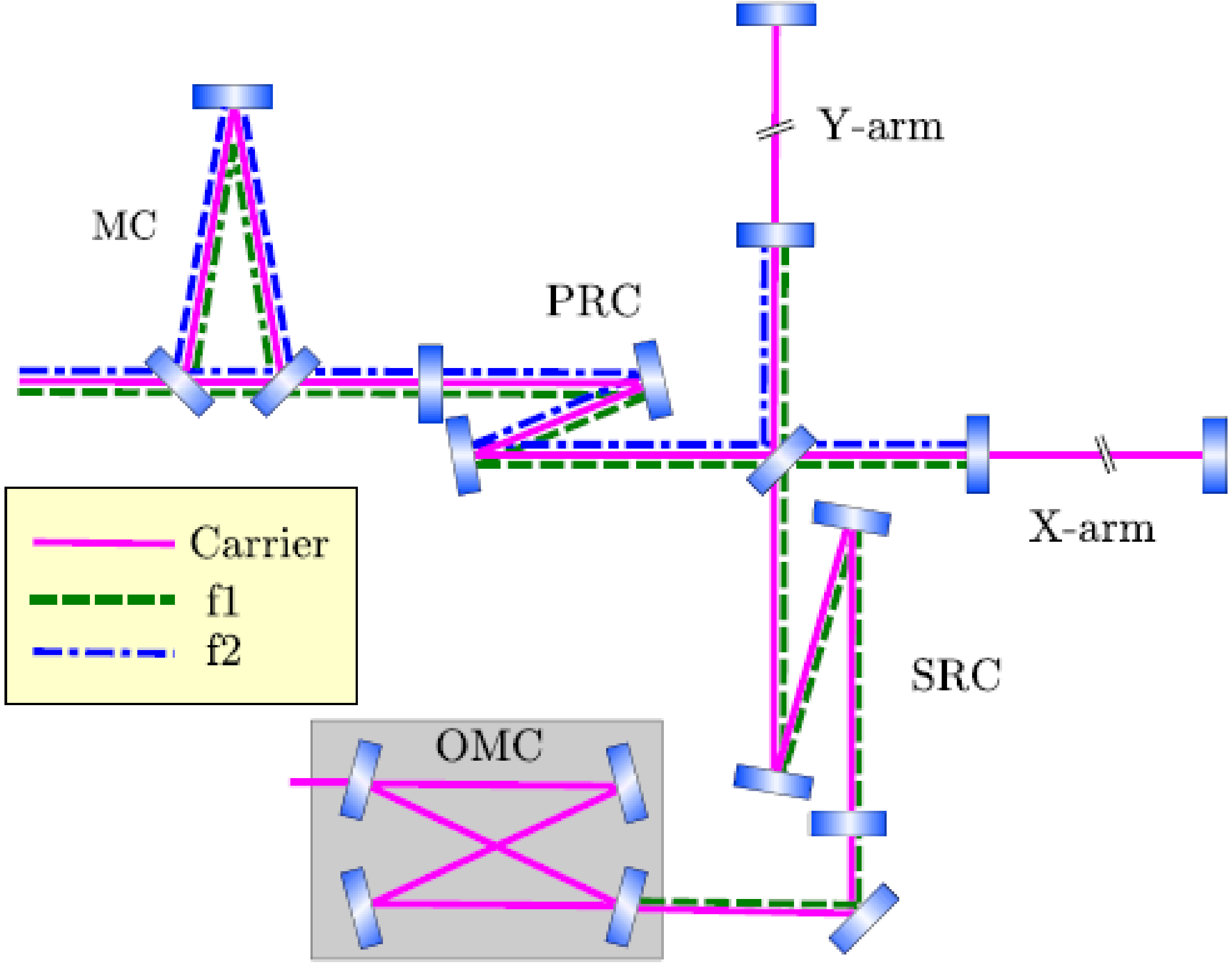

Ground-based GW detectors

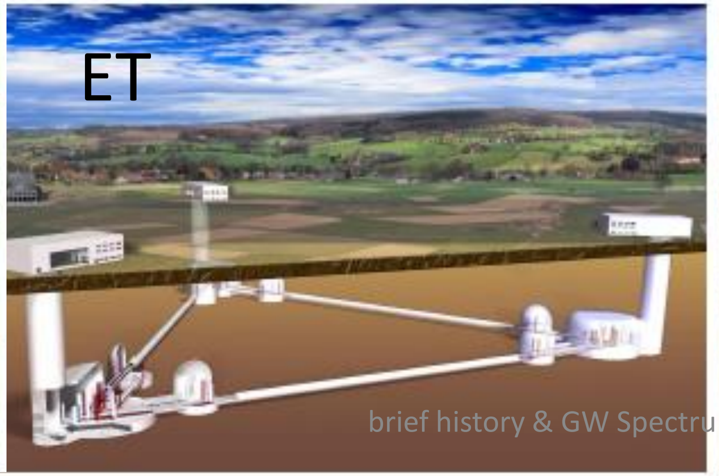

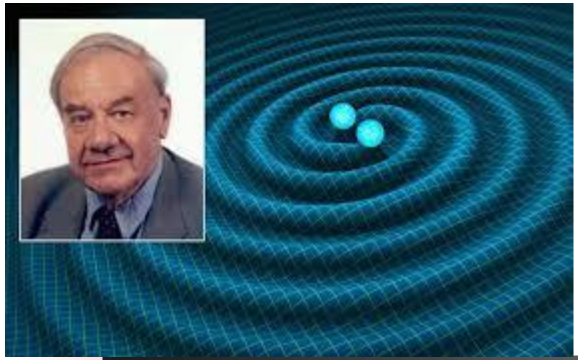

Weiss, Thorne, Drever, Giazotto and Barish

- 1970年代，Weiss 在 MIT 建立 1.5 m 的干涉仪实验研究其噪声和灵敏度，并设法劝说 Caltech 的Thorne 推动公里级探测引力波的雷射干涉仪。
- Thorne 也认为实验探测引力波重要，说动了物理系推动引力波实验，向世界公开征求一位实验主持人，选中了在 Glasgow 大学建造 1 m Fabry-Perot 干涉仪原型的 Drever (1931.10.26 – 2017.3.7.) 到 Caltech 主持建造 40 m 的 Fabry-Perot 干涉仪原型。
- 1980年代，MIT, Caltech 前后向 NSF 申请提出了 km 级臂长探测引力波的雷射干涉仪计划。
- 因大计划主持产生问题，待问题解决后，选中新主持人 Barish，始成功的获得了批准，动工建造。
- Adalberto Giazotto (1940.2.1.-2017.11.16) led the development of Virgo, emphasized the lower frequency sensitivity and led the construction of the Super Attenuator.

2016年2月11日宣布首探 Announcement of first detection

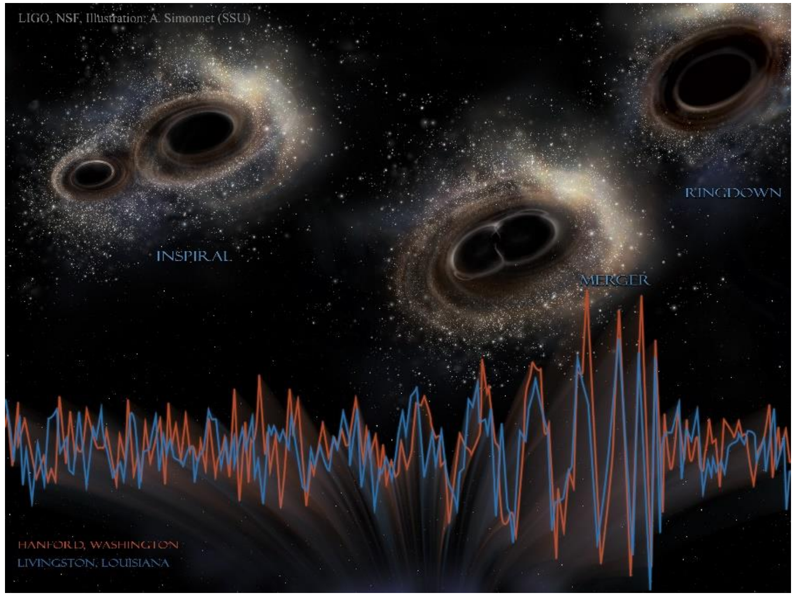

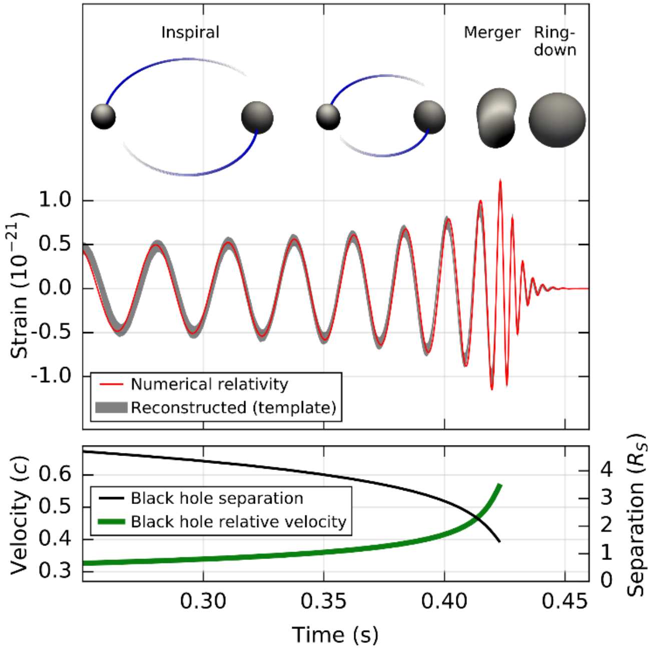

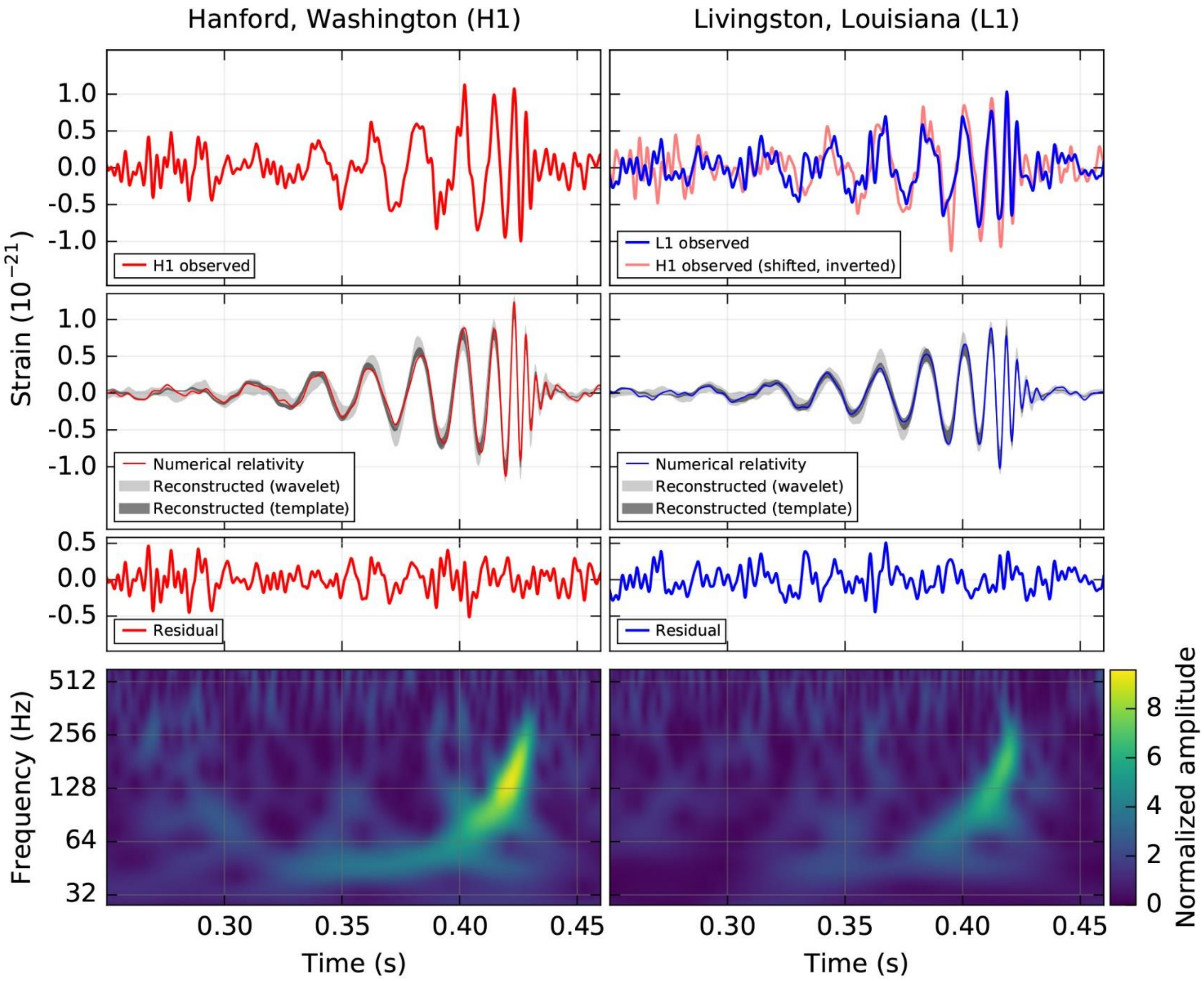

2016年6月15日宣布二探 Announcement of second detection

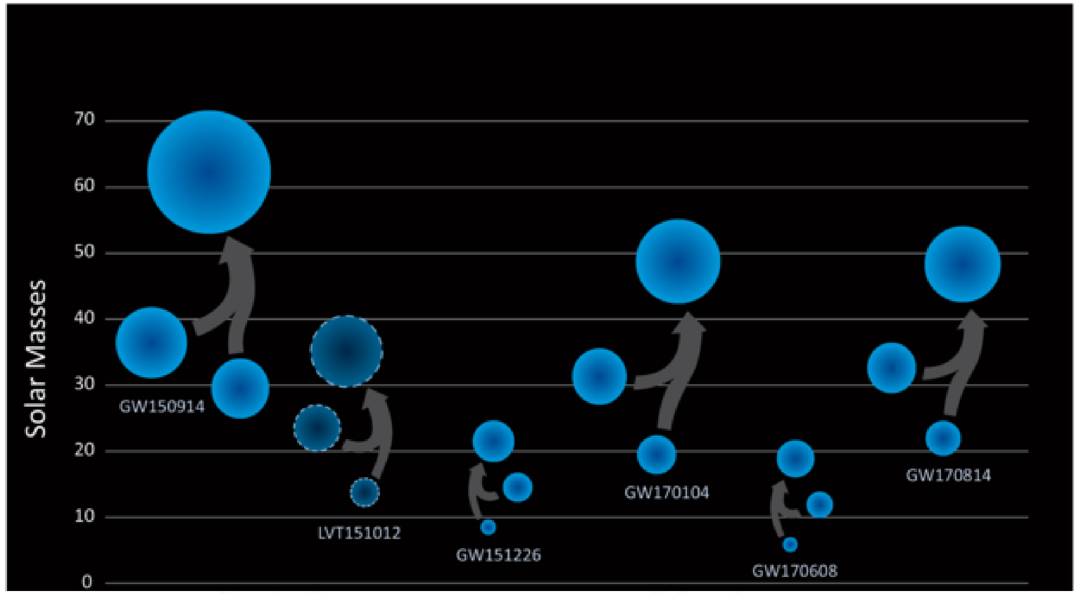

- GW151226 detected by the LIGO on December 26, 2015 at 03:38:53 UTC.
- identified within 70 s by an online matched-filter search targeting binary coalescences.
- GW151226 with S/N ratio of 13 and significance > 5σ.
- The signal ~ 1 s, about 55 cycles from 35 to 450 Hz, reached 3.4 (+0.7,−0.9) × 10^(−22). source-frame initial BH masses: 14.2 (+8.3,−3.7)$M_\odot$ and 7.5 (+2.3,−2.3)$M_\odot$, the final BH mass is 20.8 (+6.1,−1.7)$M_\odot$.
- 1 BH has spin greater than 0.2. luminosity distance 440 (+180,−190) Mpc redshift of 0.09 (+0.03,−0.04). **2σ**
- improved constraints on stellar populations and on deviations from general relativity.

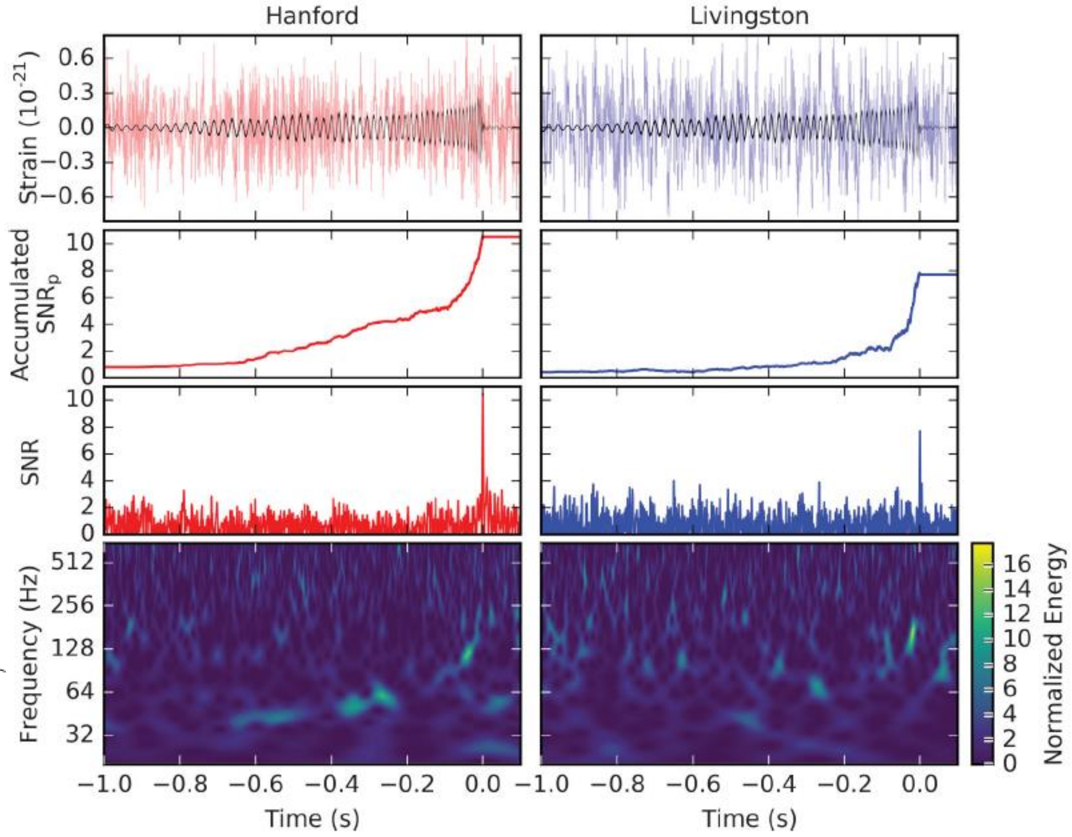

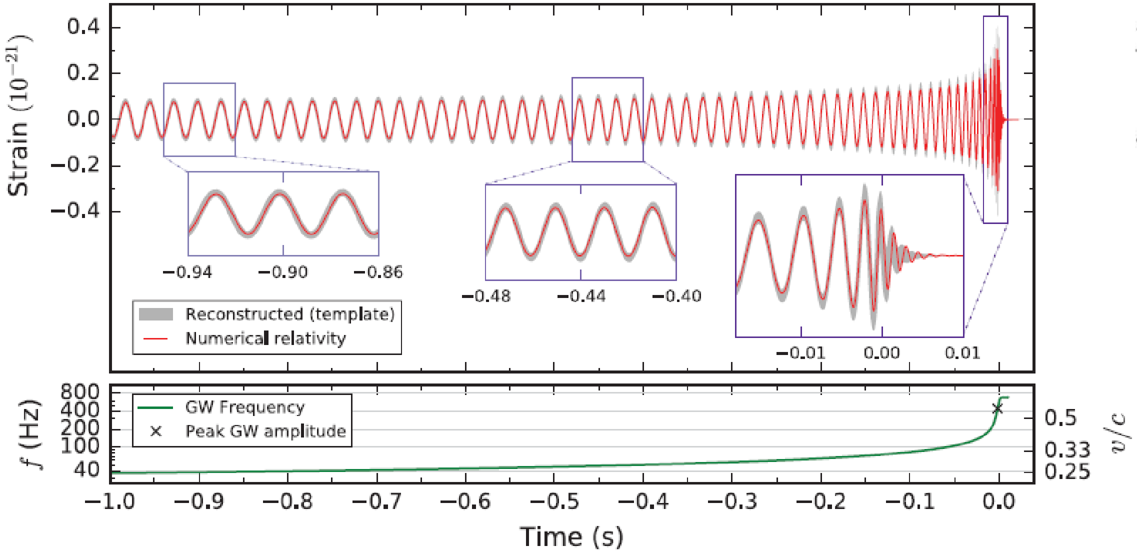

Advanced LIGO第一次观测时期：

2015.9.12—2016.1.19 (51.5天-2 detectors/130天)

O1: 48.6天; PyCBC 46.1天; GstLAL 48.3天

Event	GW150914	GW151226	LVT151012
Signal-to-noise ratio ρ	23.7	13.0	9.7
False alarm rate FAR/yr^{-1}	$< 6.0 \times 10^{-7}$	$< 6.0 \times 10^{-7}$	0.37
p-value	7.5×10^{-8}	7.5×10^{-8}	0.045
Significance	$> 5.3\sigma$	$> 5.3\sigma$	1.7σ
Primary mass $m_1^{\mathrm{source}}/\mathrm{M}_\odot$	$36.2^{+5.2}_{-3.8}$	$14.2^{+8.3}_{-3.7}$	23^{+18}_{-6}
Secondary mass $m_2^{\mathrm{source}}/\mathrm{M}_\odot$	$29.1^{+3.7}_{-4.4}$	$7.5^{+2.3}_{-2.3}$	13^{+4}_{-5}
Chirp mass $\mathscr{M}^{\mathrm{source}}/\mathrm{M}_\odot$	$28.1^{+1.8}_{-1.5}$	$8.9^{+0.3}_{-0.3}$	$15.1^{+1.4}_{-1.1}$
Total mass $M^{\mathrm{source}}/\mathrm{M}_\odot$	$65.3^{+4.1}_{-3.4}$	$21.8^{+5.9}_{-1.7}$	37^{+13}_{-4}
Effective inspiral spin χ_{eff}	$-0.06^{+0.14}_{-0.14}$	$0.21^{+0.20}_{-0.10}$	$0.0^{+0.3}_{-0.2}$
Final mass $M_{\mathrm{f}}^{\mathrm{source}}/\mathrm{M}_\odot$	$62.3^{+3.7}_{-3.1}$	$20.8^{+6.1}_{-1.7}$	35^{+14}_{-4}
Final spin a_{f}	$0.68^{+0.05}_{-0.06}$	$0.74^{+0.06}_{-0.06}$	$0.66^{+0.09}_{-0.10}$
Radiated energy $E_{\mathrm{rad}}/(\mathrm{M}_\odot c^2)$	$3.0^{+0.5}_{-0.4}$	$1.0^{+0.1}_{-0.2}$	$1.5^{+0.3}_{-0.4}$
Peak luminosity $\ell_{\mathrm{peak}}/(\mathrm{erg\,s}^{-1})$	$3.6^{+0.5}_{-0.4} \times 10^{56}$	$3.3^{+0.8}_{-1.6} \times 10^{56}$	$3.1^{+0.8}_{-1.8} \times 10^{56}$
Luminosity distance $D_{\mathrm{L}}/\mathrm{Mpc}$	420^{+150}_{-180}	440^{+180}_{-190}	1000^{+500}_{-500}
Source redshift z	$0.09^{+0.03}_{-0.04}$	$0.09^{+0.03}_{-0.04}$	$0.20^{+0.09}_{-0.09}$
Sky localization $\Delta\Omega/\mathrm{deg}^2$	230	850	1600

Amplitude spectral density and Wave forms of 3 detected signals

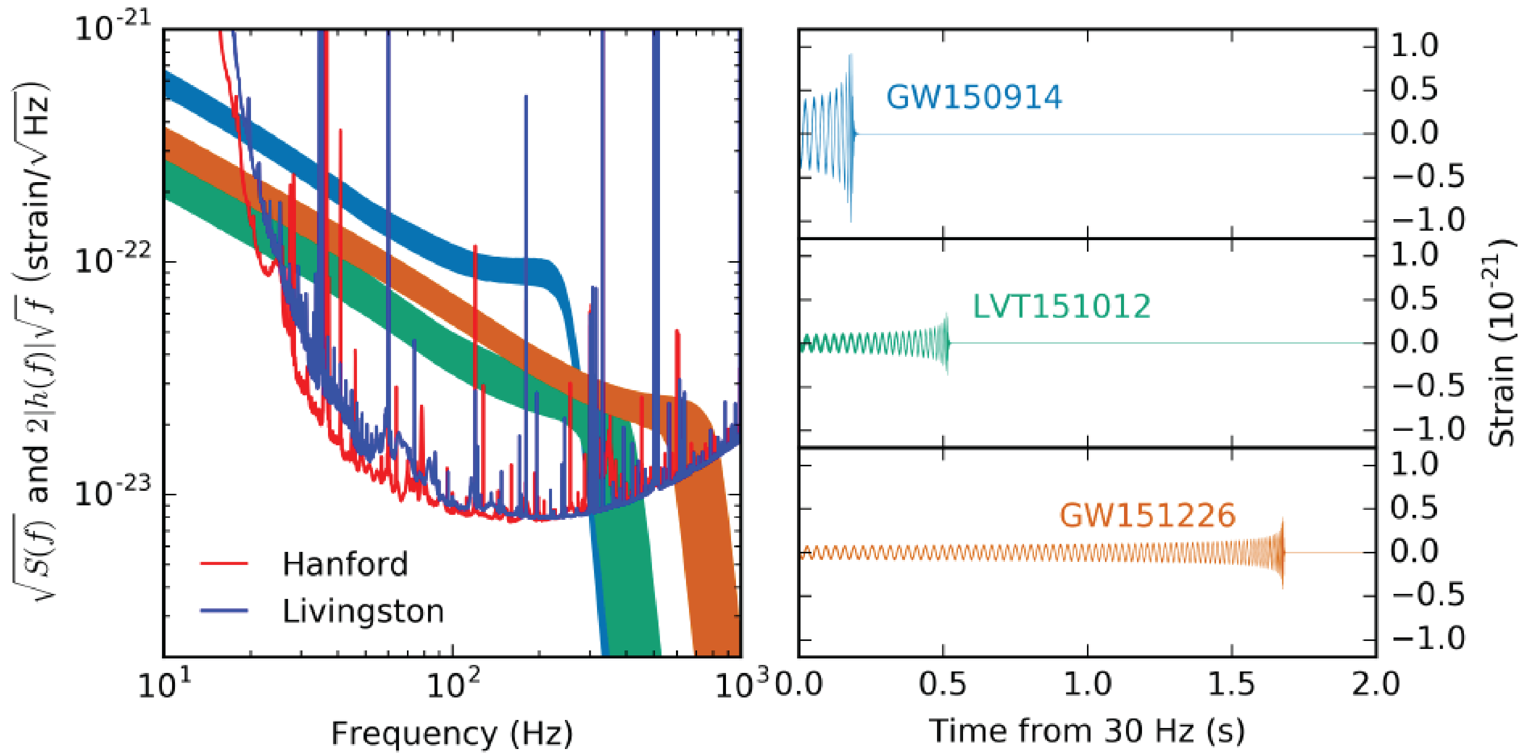

GW170814

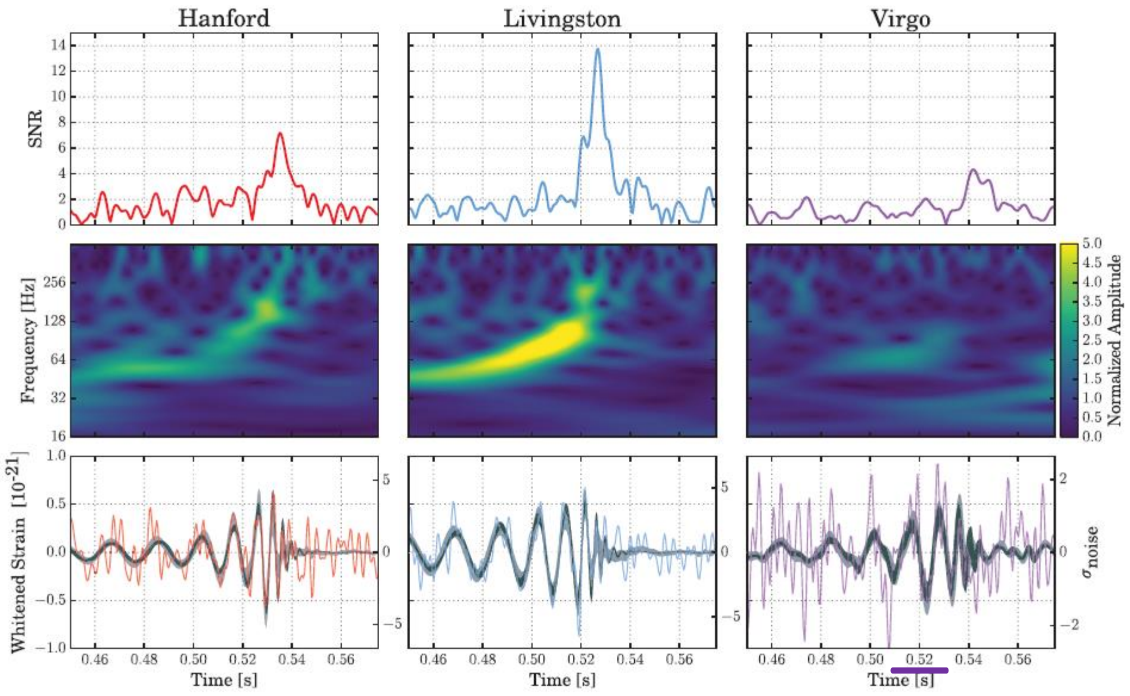

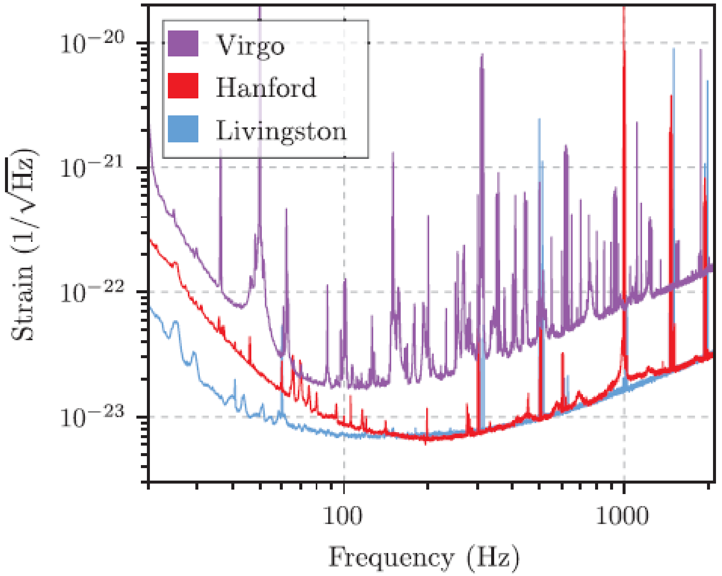

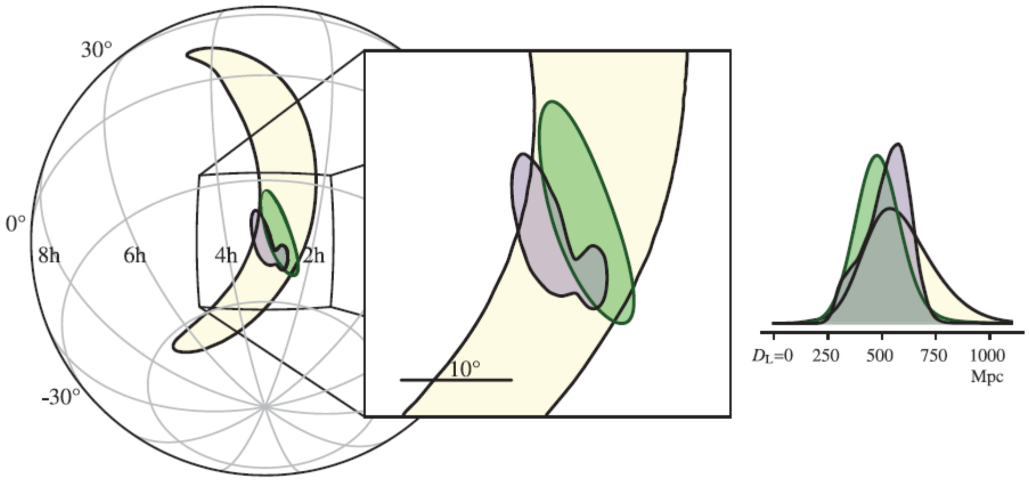

Primary black hole mass m_1	$30.5^{+5.7}_{-3.0} M_\odot$
Secondary black hole mass m_2	$25.3^{+2.8}_{-4.2} M_\odot$
Chirp mass $\mathcal{M}$	$24.1^{+1.4}_{-1.1} M_\odot$
Total mass M	$55.9^{+3.4}_{-2.7} M_\odot$
Final black hole mass M_f	$53.2^{+3.2}_{-2.5} M_\odot$
Radiated energy E_{rad}	$2.7^{+0.4}_{-0.3} M_\odot\ c^2$
Peak luminosity ℓ_{peak}	$3.7^{+0.5}_{-0.5} \times 10^{56}\ \mathrm{erg\,s^{-1}}$
Effective inspiral spin parameter χ_{eff}	$0.06^{+0.12}_{-0.12}$
Final black hole spin a_f	$0.70^{+0.07}_{-0.05}$
Luminosity distance D_L	540^{+130}_{-210} Mpc
Source redshift z	$0.11^{+0.03}_{-0.04}$

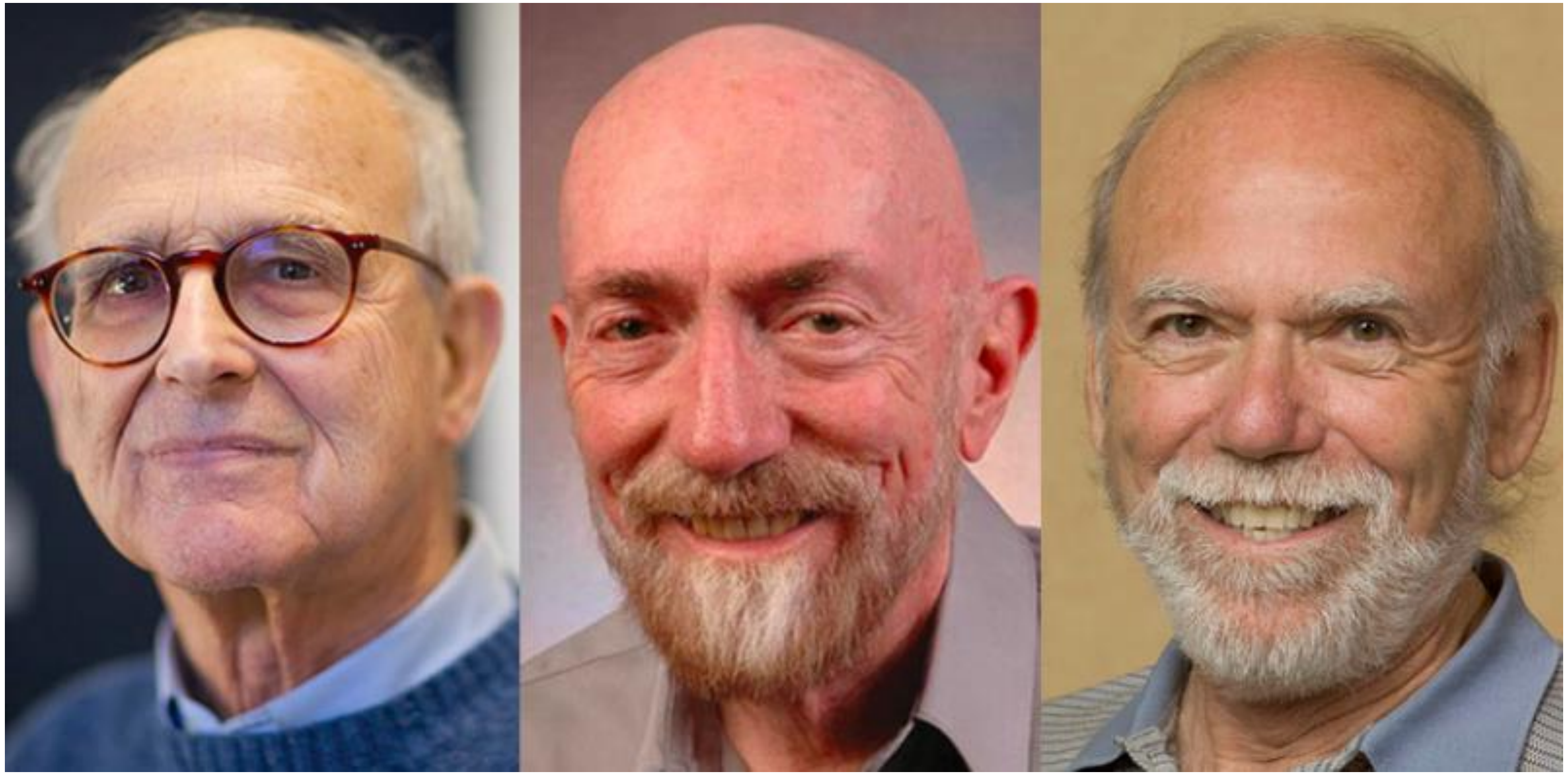

- 2017 诺贝尔物理奖发表啰，得奖者是 85 岁的莱纳·魏斯（Rainer Weiss）、77 岁的基普·索恩（Kip S. Thorne）、81 岁的巴瑞·巴利许（Barry Barish），他们因为 LIGO 探测器及重力波探测的成就而获奖，三人将共享高达 900 万瑞典克朗（约 3,346 万元台币）的奖金。

GW170817
中子双星合生

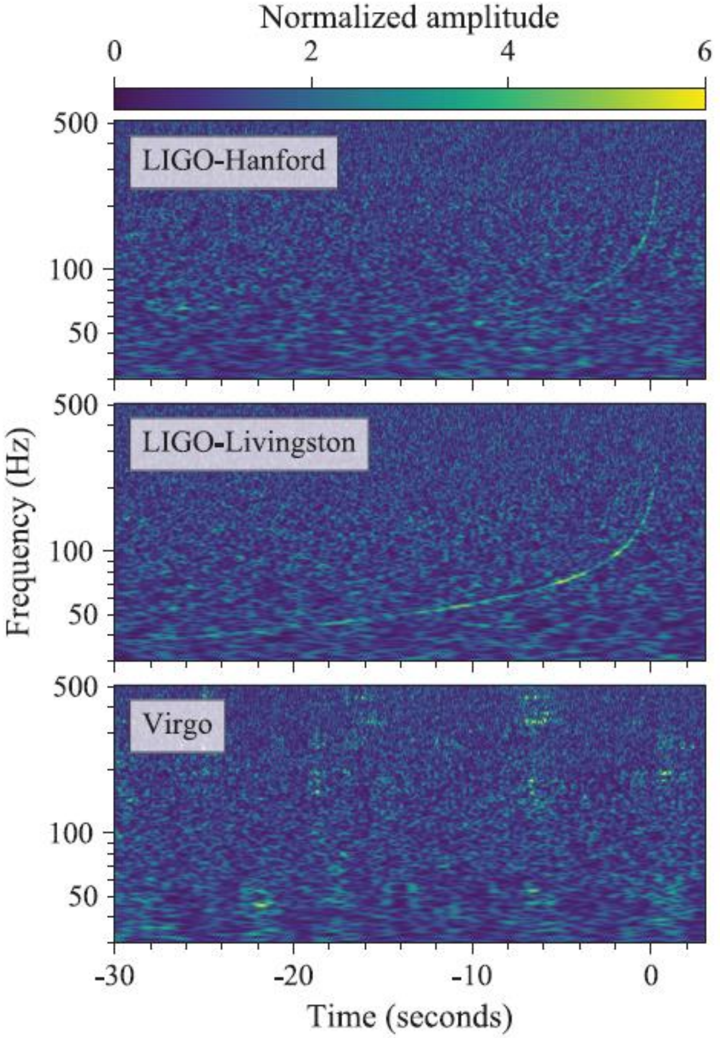

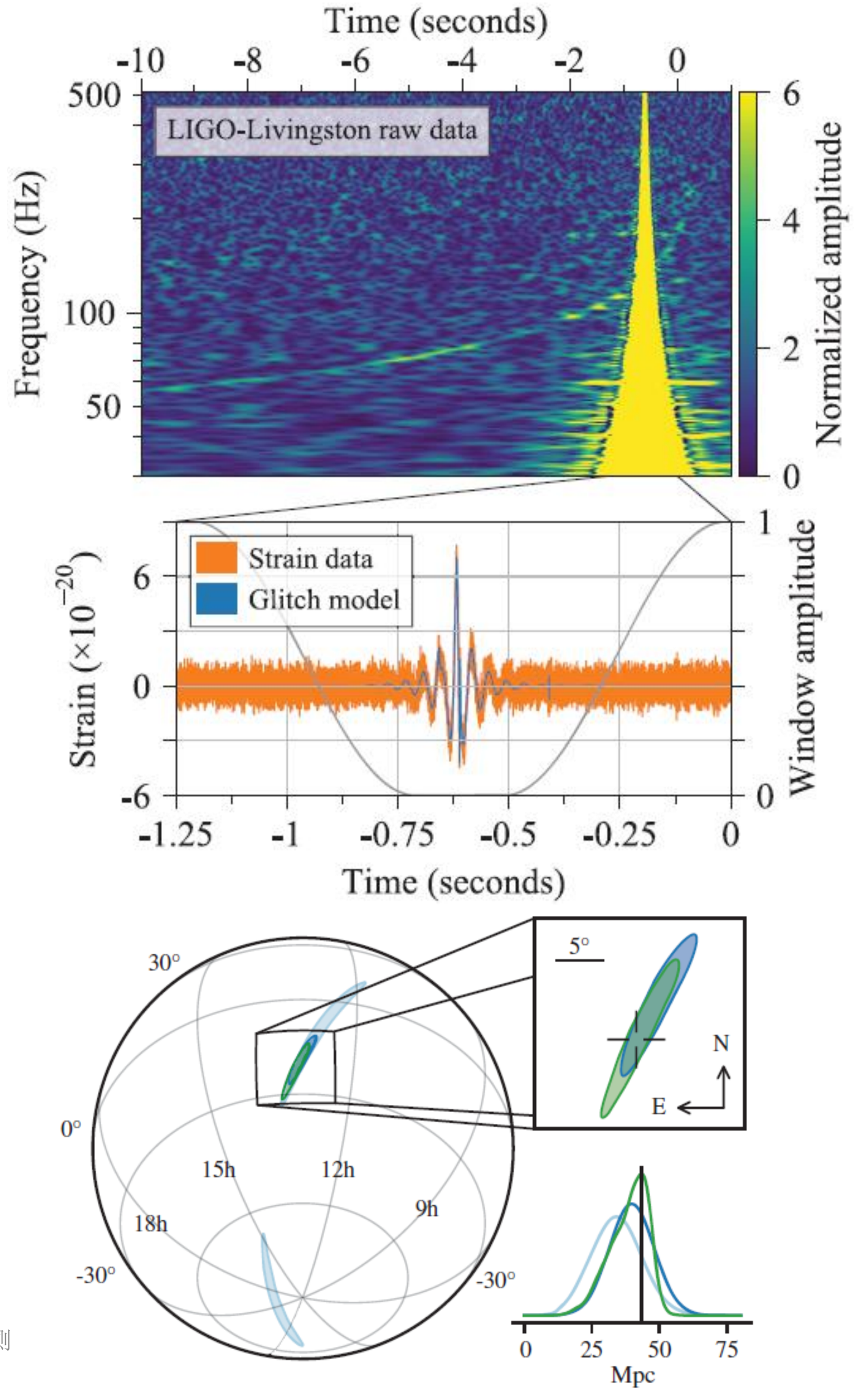

GW170817 中子双星合生

	Low-spin priors ($\|\chi\| \leq 0.05$)	High-spin priors ($\|\chi\| \leq 0.89$)
Primary mass m_1	$1.36–1.60\ M_\odot$	$1.36–2.26\ M_\odot$
Secondary mass m_2	$1.17–1.36\ M_\odot$	$0.86–1.36\ M_\odot$
Chirp mass $\mathcal{M}$	$1.188^{+0.004}_{-0.002} M_\odot$	$1.188^{+0.004}_{-0.002} M_\odot$
Mass ratio m_2/m_1	0.7–1.0	0.4–1.0
Total mass $m_{\rm tot}$	$2.74^{+0.04}_{-0.01} M_\odot$	$2.82^{+0.47}_{-0.09} M_\odot$
Radiated energy $E_{\rm rad}$	$> 0.025 M_\odot c^2$	$> 0.025 M_\odot c^2$
Luminosity distance $D_{\rm L}$	40^{+8}_{-14} Mpc	40^{+8}_{-14} Mpc
Viewing angle Θ	$\leq 55°$	$\leq 56°$
Using NGC 4993 location	$\leq 28°$	$\leq 28°$
Combined dimensionless tidal deformability $\tilde{\Lambda}$	≤ 800	≤ 700
Dimensionless tidal deformability $\Lambda(1.4 M_\odot)$	≤ 800	≤ 1400

多信使天文学观测

引力波与伽玛暴

GRB170817A 比 GW170817

晚1.74 ± 0.05秒到达地球

重力波速度和光速相同的精度

$-3\times10^{-15} \leq (\Delta v/c_{EM}) \leq 7\times10^{-16}$

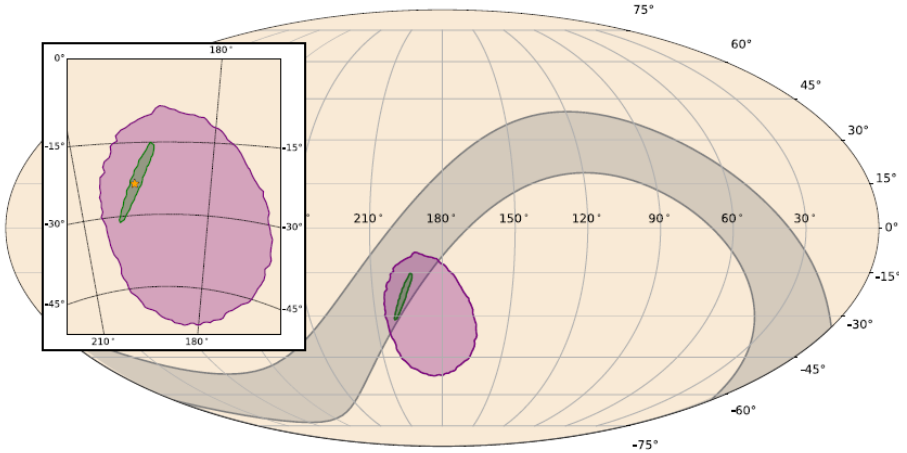

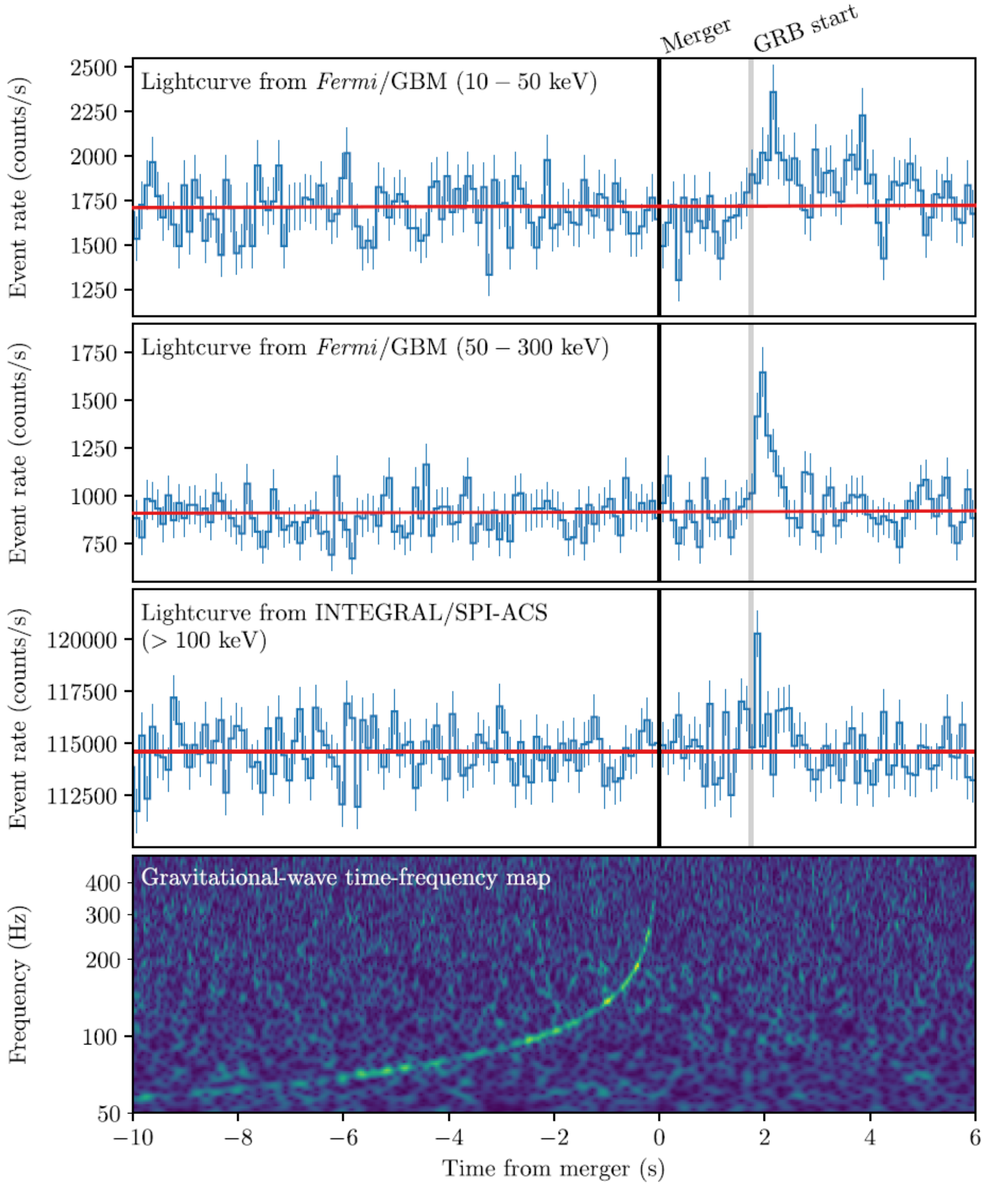

The Origin of the Solar System Elements

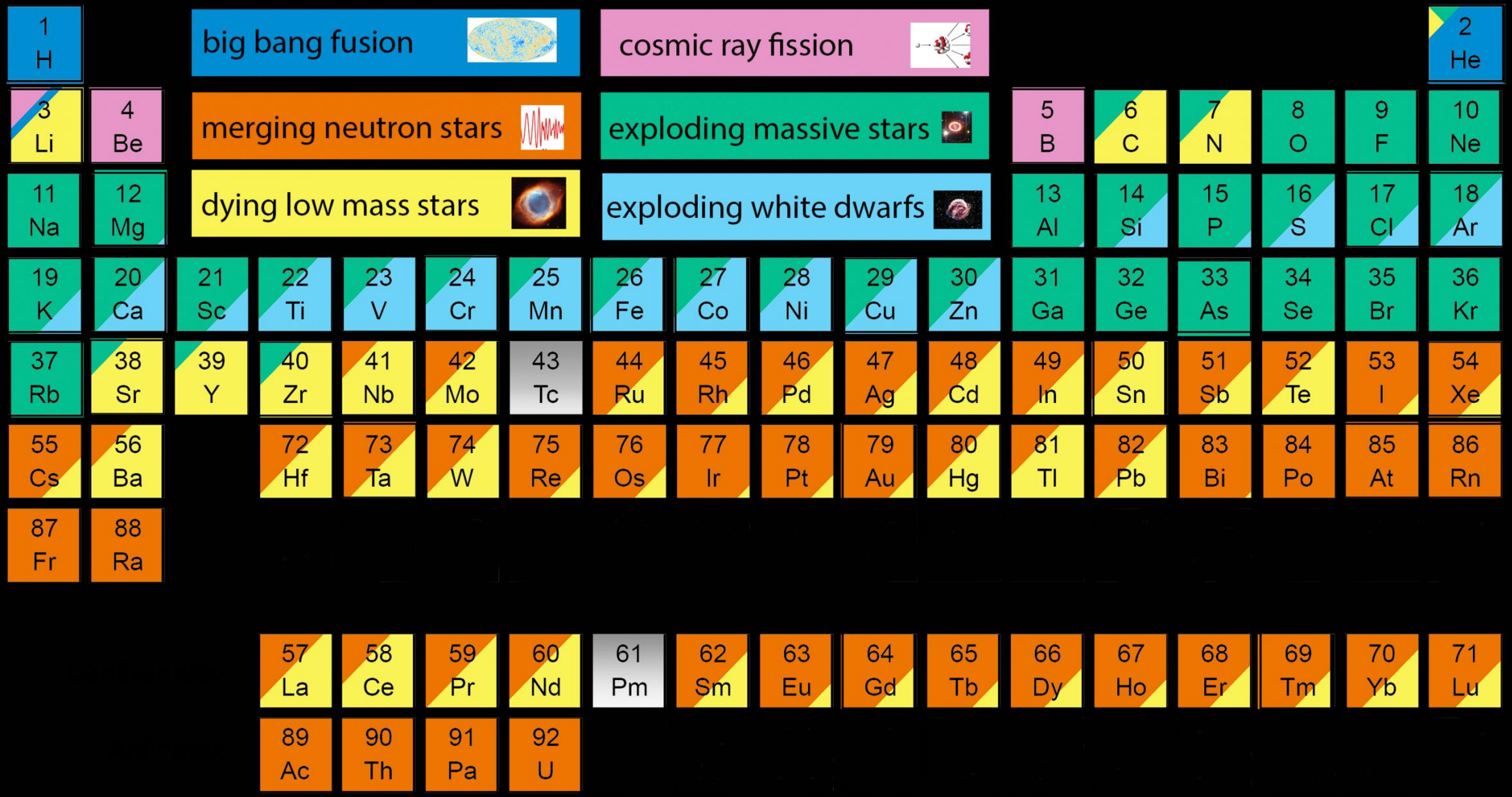

黑洞大小分类Massive Black Hole Systems: Massive BH Mergers & Extreme Mass Ratio Mergers (EMRIs)

- 恒星质量黑洞*Stellar-mass BHs* (3$M_\odot$ < *M*BH ≤ 100$M_\odot$)
- 超大质量黑洞*Supermassive BHs* (*SMBHs*; *M*BH ≥ $10^6 M_\odot$)
- 中级质量黑洞*Intermediate-mass BHs* (*IMBHs*; 100$M_\odot$ < *M*BH < $10^6 M_\odot$)

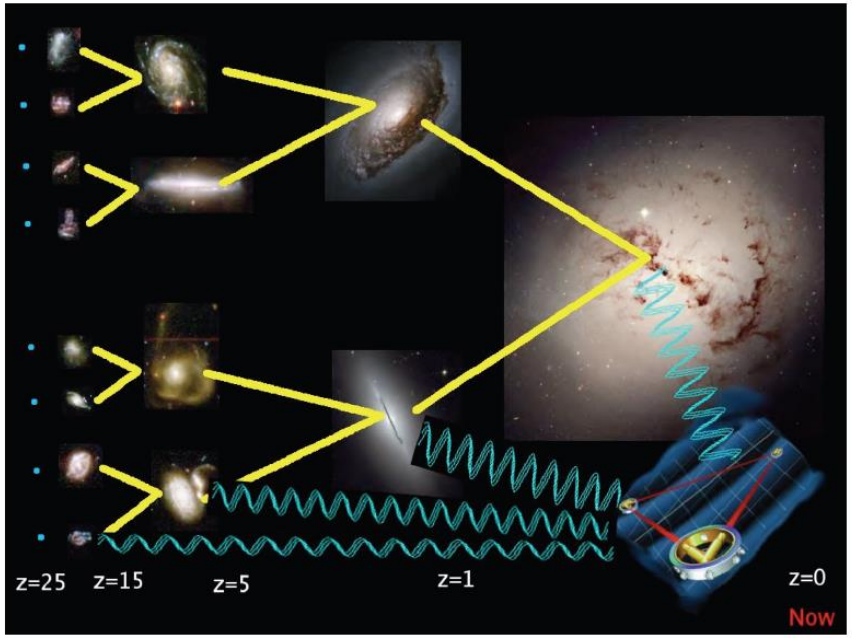

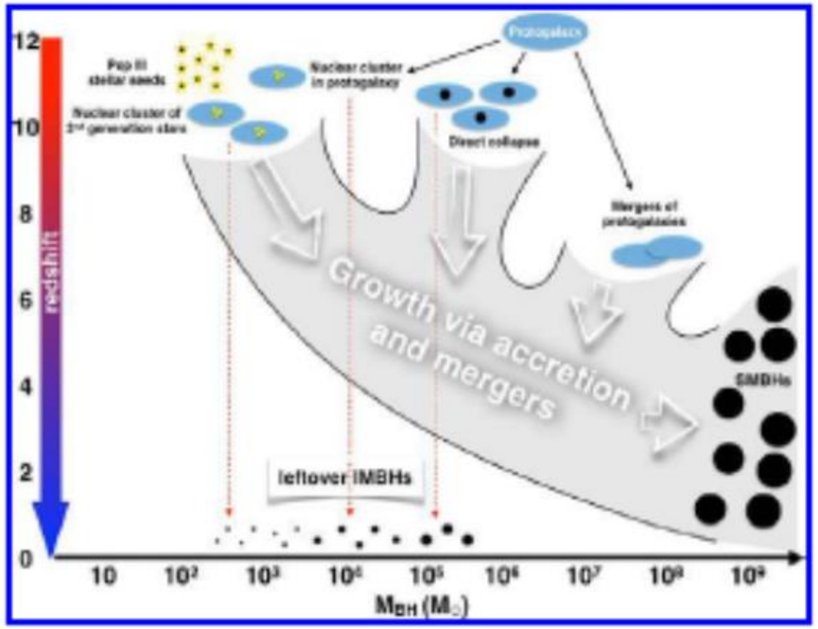

Scope: Goals –GW Astronomy & Fundamental Physics

Frequency band	GW sources / Possible GW sources	Detection method
Ultrahigh frequency band: above 1 THz	Discrete sources, Cosmological sources, Braneworld Kaluza-Klein (KK) mode radiation, Plasma instabilities	Terahertz resonators, optical resonators, and magnetic conversion detectors
Very high frequency band: 100 kHz – 1 THz	Discrete sources, Cosmological sources, Braneworld Kaluza-Klein (KK) mode radiation, Plasma instabilities	Microwave resonator/wave guide detectors, laser interferometers and Gaussian beam detectors
High frequency band (audio band)*: 10 Hz – 100 kHz	Compact binaries [NS (Neutron Star)-NS, NS-BH (Black Hole), BH-BH], Supernovae	Low-temperature resonators and Earth-based laser-interferometric detectors
Middle frequency band: 0.1 Hz – 10 Hz	Intermediate mass black hole binaries, massive star (population III star) collapses	Space laser-interferometric detectors of arm length 1,000 km − 60,000 km
Low frequency band (milli-Hz band)†: 100 nHz – 0.1 Hz	Massive black hole binaries, Extreme mass ratio inspirals (EMRIs), Compact binaries	Space laser-interferometric detectors of arm length longer than 60,000 km
Very low frequency band (nano-Hz band): 300 pHz – 100 nHz	Supermassive black hole binary (SMBHB) coalescences, Stochastic GW background from SMBHB coalescences	Pulsar timing arrays (PTAs)
Ultralow frequency band: 10 fHz – 300 pHz	Inflationary/primordial GW background, Stochastic GW background	Astrometry of quasar proper motions
Extremely low (Hubble) frequency band: 1 aHz–10 fHz	Inflationary/primordial GW background	Cosmic microwave background experiments
Beyond Hubble-frequency band: below 1 aHz	Inflationary/primordial GW background	Through the verifications of primordial cosmological models

引力波谱分类 The Gravitation-Wave (GW) Spectrum Classification

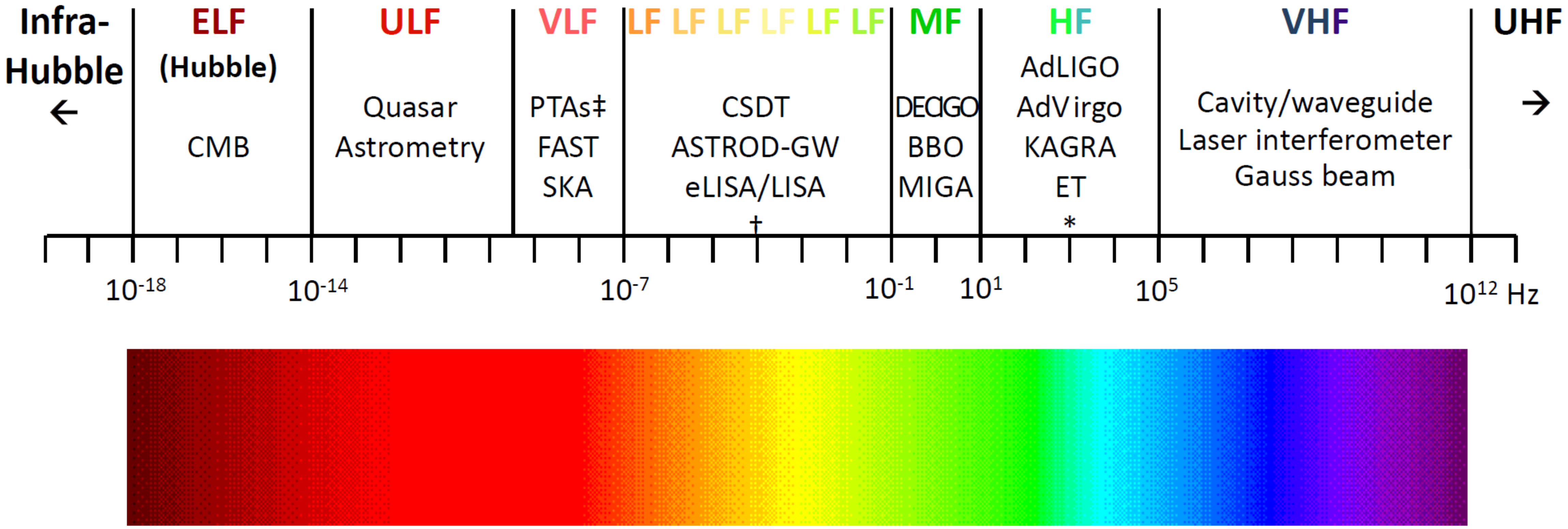

* AIGO, AURIGA, EXPLORER, GEO, NAUTILUS, MiniGRAIL, Schenberg.

† OMEGA, gLISA/GEOGRAWI, GADFLI, TIANQIN, ASTROD-EM, LAGRANGE, ALIA, ALIA-descope.

‡ EPTA, NANOGrav, PPTA, IPTA.

Cosmic band slow-roll model r=0.07, n_t=-r/8

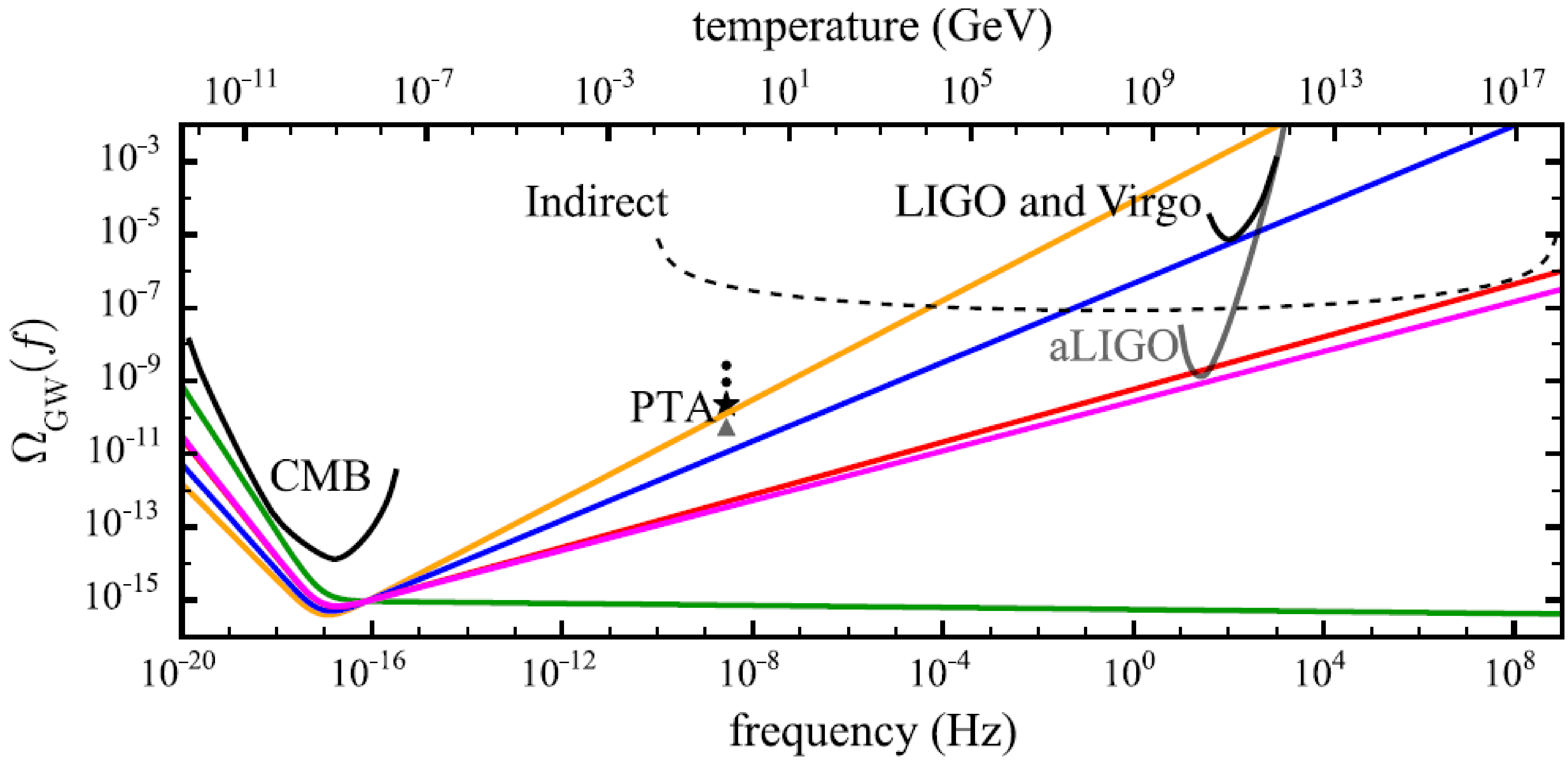

Normalized GW spectral energy density Ω_{gw} vs. frequency for GW detector sensitivities and GW sources

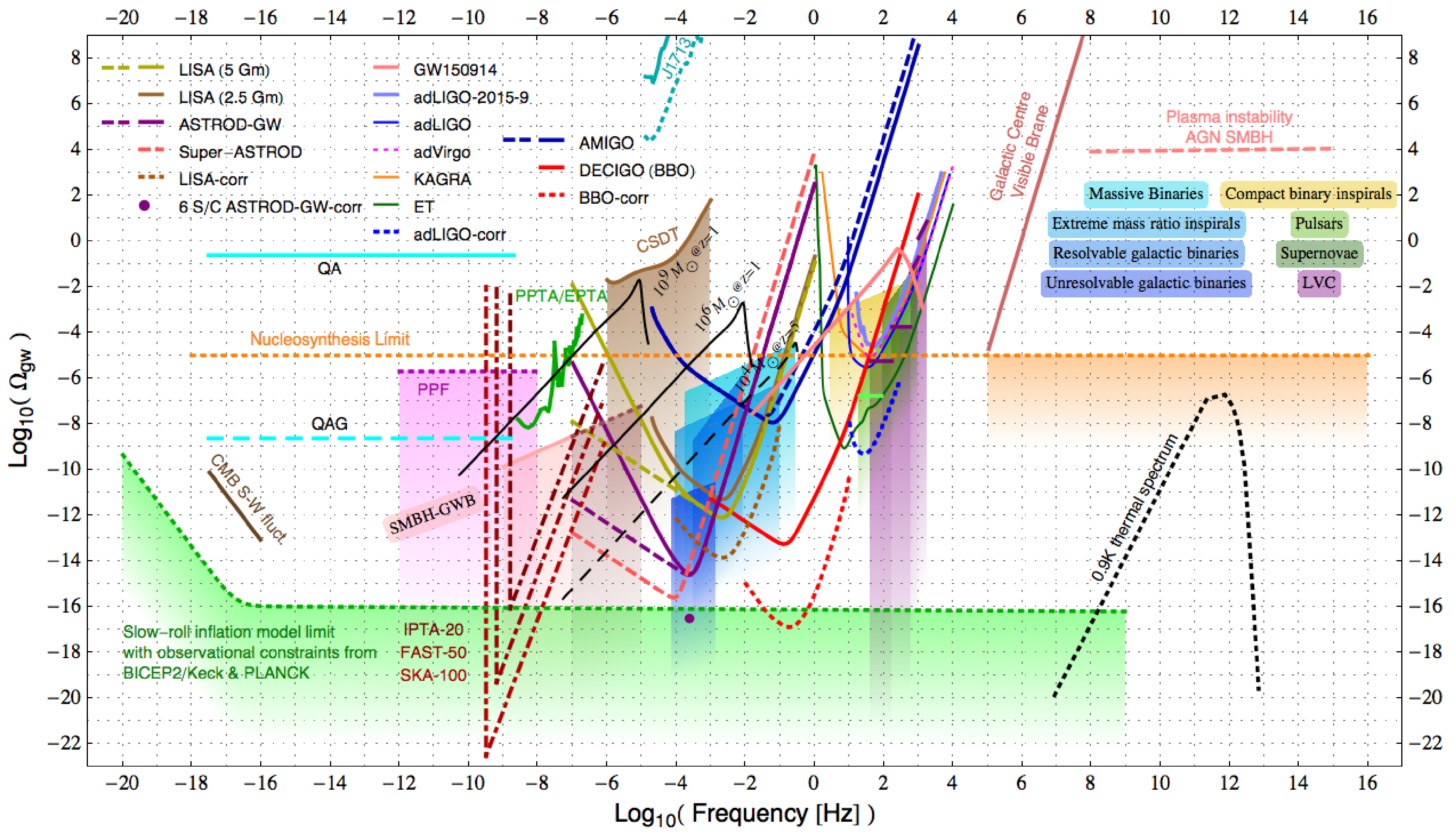

Very low frequency band (300 pHz – 100 nHz)

$$h_c(f) = A_{\rm yr}\,[f/(1\ {\rm yr}^{-1})]^{\alpha}$$

Table 4. Upper limits on the isotropic stochastic background from 3 pulsar timing arrays.

	No. of pulsars included	No. of years observed	Observation radio band [MHz]	Constraint on characteristic strain $h_c(f)$ [$= A_{\rm yr}\,[f/(1{\rm yr}^{-1})]^{-(2/3)}$, ($f = 10^{-9}$-$10^{-7}$ Hz)]
EPTA[102]	6	18	120-3000	$A_{\rm yr} < 3 \times 10^{-15}$
PPTA[103]	4	11	3100	$A_{\rm yr} < 1 \times 10^{-15}$
NANOGrav[104]	27	9	327-2100	$A_{\rm yr} < 1.5 \times 10^{-15}$

Table 5. Sensitivities of IPTA, FAST and SKA to monochromatic GWs.

	No. of pulsars	No. of years of observation	Timing accuracy (ns)	Sensitivity in characteristic strain $h_c(f)$ [$= B_{\rm yr}\,(f / {\rm yr}^{-1})$] for monochromatic GWs
IPTA[106]	36	20	100	$B_{\rm yr} = 1 \times 10^{-16}$
FAST[107]	50	50	50	$B_{\rm yr} = 1.5 \times 10^{-17}$
SKA[108]	100	100	20	$B_{\rm yr} = 1.5 \times 10^{-18}$

Conversion factors among: the characteristic strain $h_c(f)$, the strain psd (power spectral density) $[S_h(f)]^{1/2}$ the normalized spectral energy density $\Omega_{gw}(f)$

- $h_c(f) = f^{1/2}\,[S_h(f)]^{1/2}$;
- *normalized GW spectral energy density* $\Omega_g(f)$: GW spectral energy density in terms of *the energy density per logarithmic frequency interval divided by the cosmic closure density* ρ_c for a cosmic GW sources or background, i.e.,
- $\Omega_{gw}(f) = (f/\rho_c)\,\mathrm{d}\rho(f)/\mathrm{d}f$
- $\Omega_{gw}(f) = (2\pi^2/3H_0^2)\,f^3\,S_h(f) = (2\pi^2/3H_0^2)\,f^2\,h_c^2(f)$.

	Characteristic strain $h_c(f)$	Strain psd $[S_h(f)]^{1/2}$	Normalized spectral energy density $\Omega_{gw}(f)$
$h_c(f)$	$h_c(f)$	$f^{1/2}\,[S_h(f)]^{1/2}$	$[(3H_0^2/2\pi^2f^2)\Omega_{gw}(f)]^{1/2}$
Strain psd $[S_h(f)]^{1/2}$	$f^{-1/2}h_c(f)$	$[S_h(f)]^{1/2}$	$[(3H_0^2/2\pi^2f^3)\Omega_{gw}(f)]^{1/2}$
$\Omega_{gw}(f)$	$(2\pi^2/3H_0^2)\,f^2\,h_c^2(f)$	$(2\pi^2/3H_0^2)\,f^3\,S_h(f)$	$\Omega_{gw}(f)$

Strain power spectral density (psd) amplitude vs. frequency for various GW detectors and GW sources

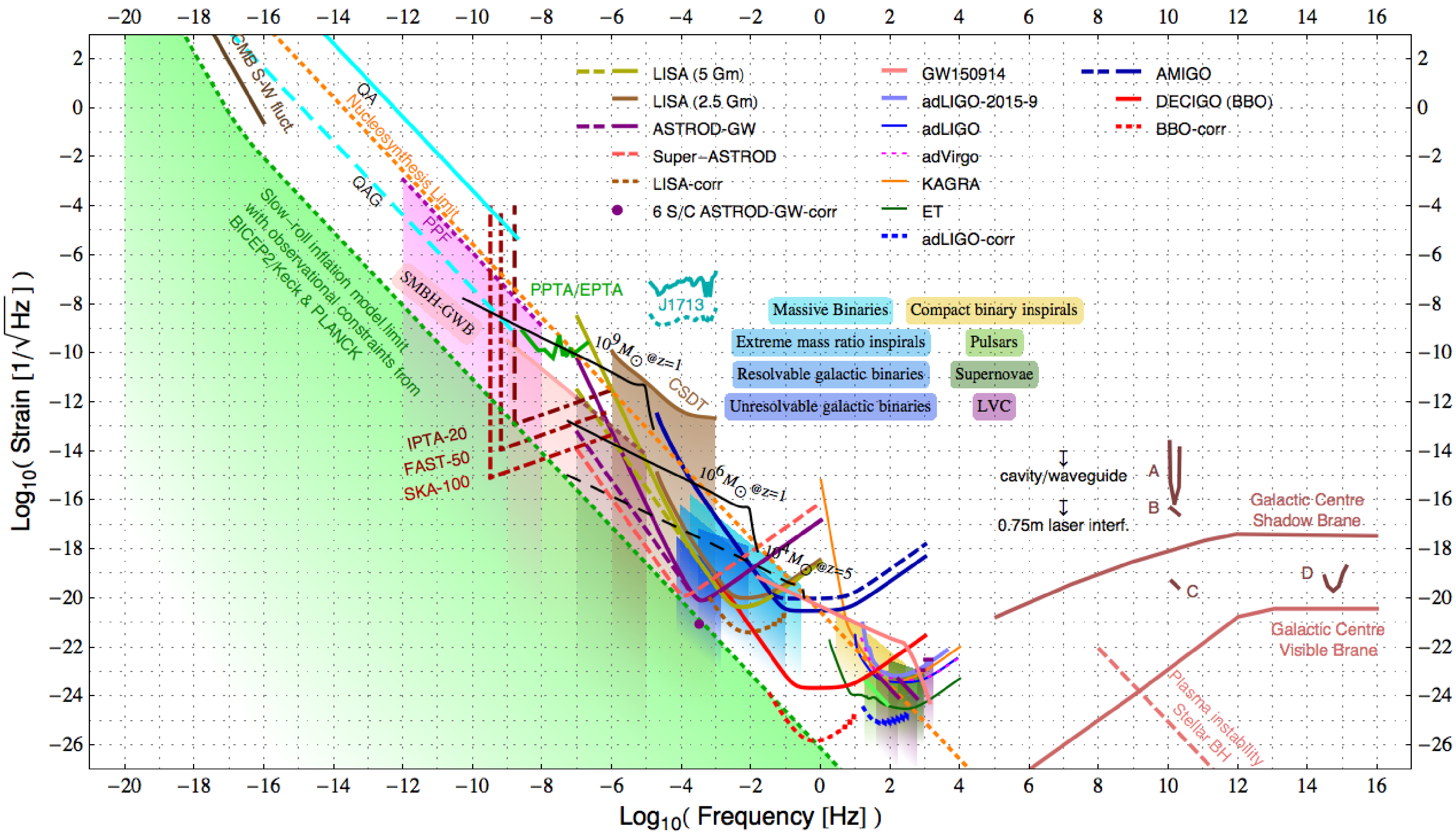

Characteristic strain h_c vs. frequency for various GW detectors and sources. [QA: Quasar Astrometry; QAG: Quasar Astrometry Goal; LVC: LIGO-Virgo Constraints; CSDT: Cassini Spacecraft Doppler Tracking; SMBH-GWB: Supermassive Black Hole-GW Background.]

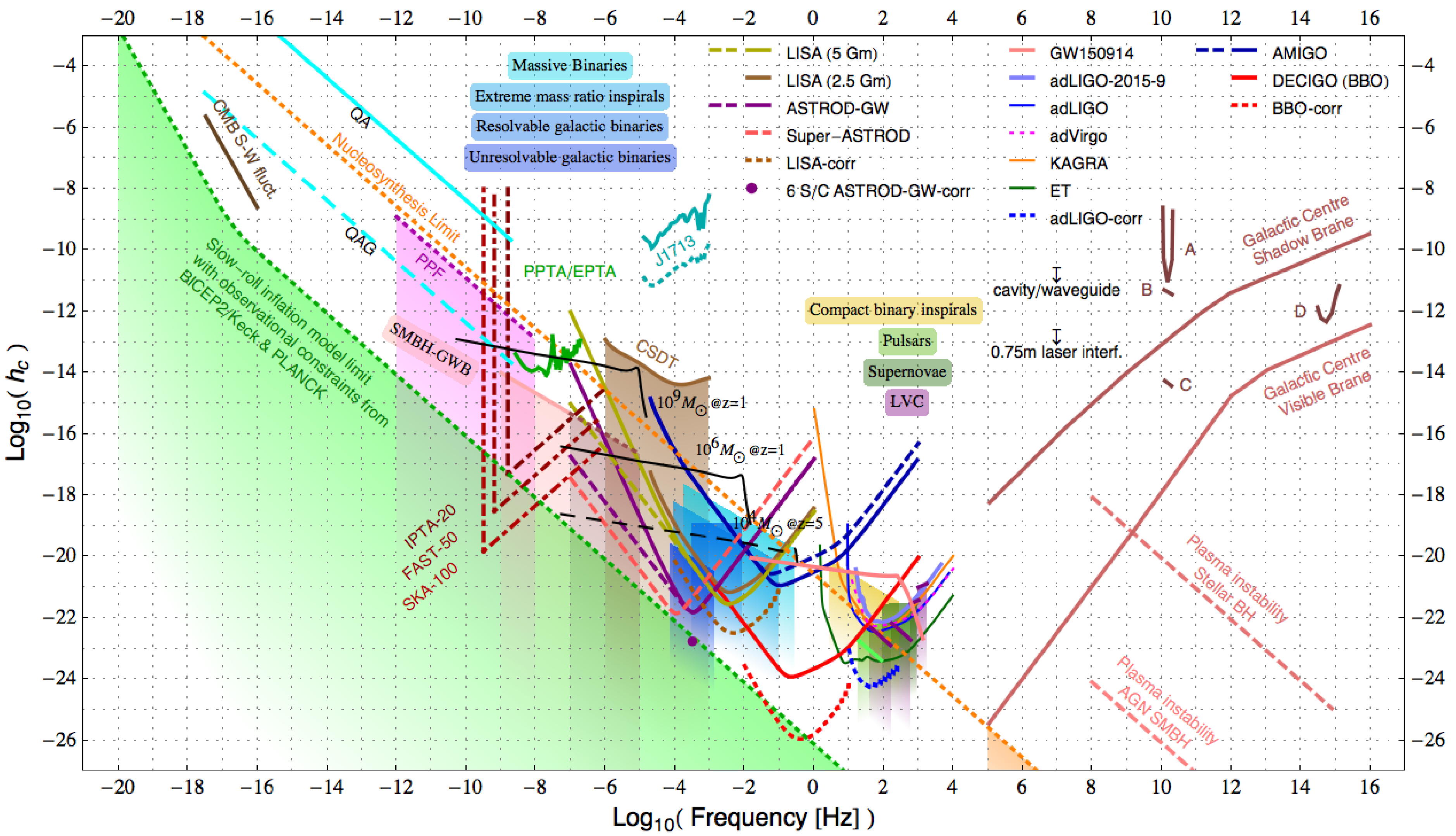

Strain power spectral density (psd) amplitude vs. frequency for various GW detectors and GW sources

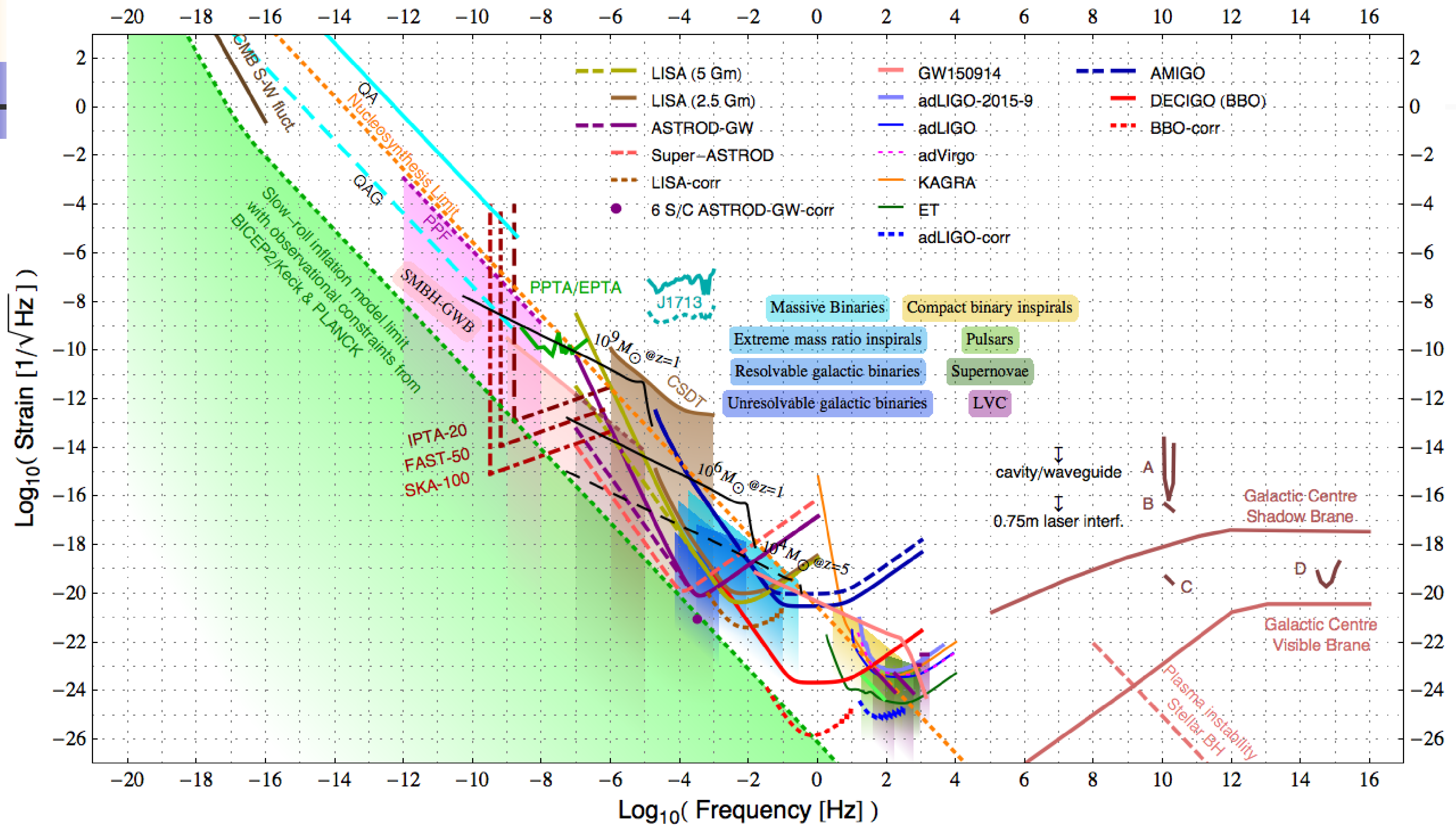

GW20150914

LIGO

LISA

(from Sesana 2017 prl)

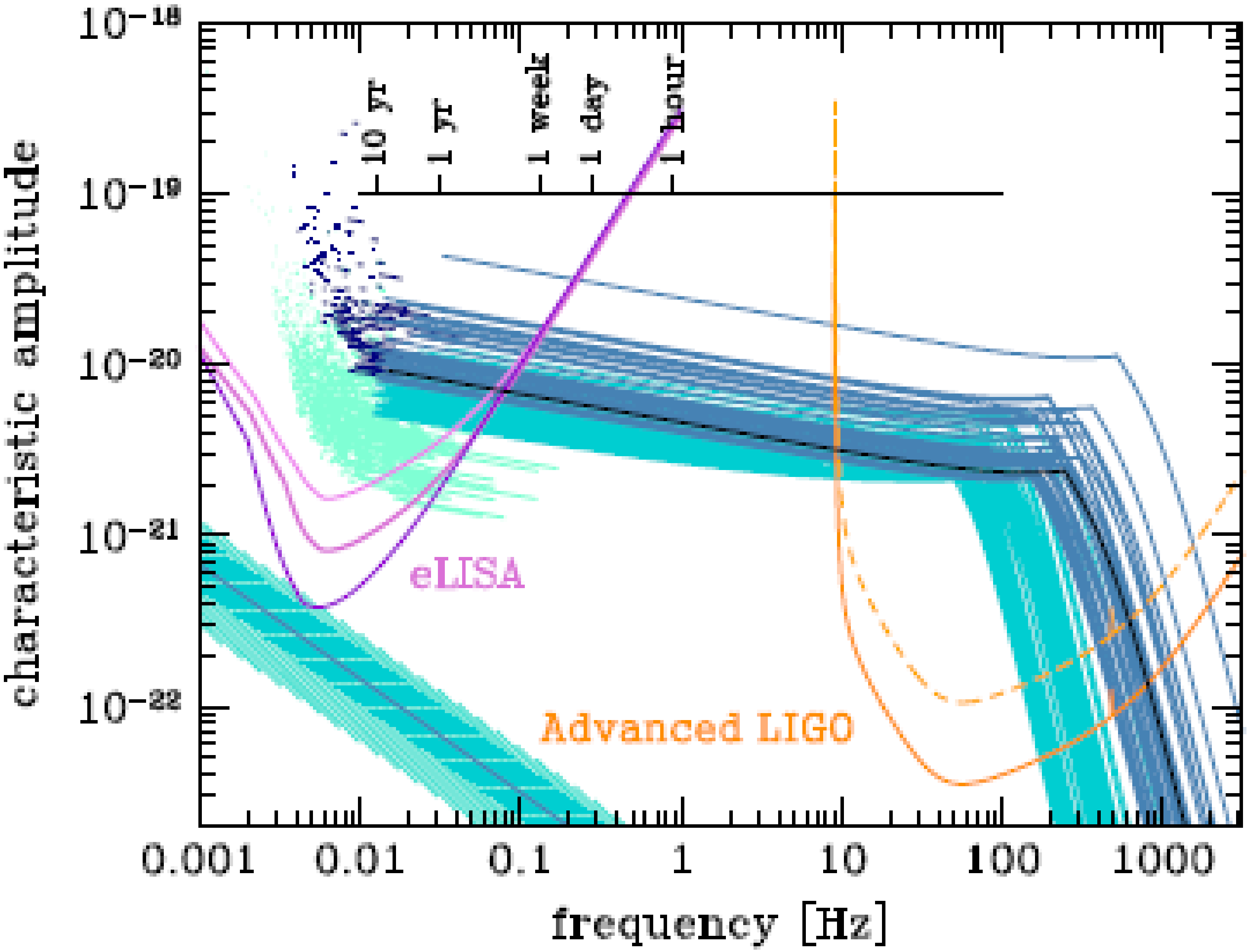

Middle frequency GW Detection Science Goals

- **The science goals are the detection of GWs from**

- **(i) Intermediate-Mass Black Holes; could detect IMBH binaries at a few billion light years away or further**
- **(ii) Galactic Compact Binaries as well as stellar mass BH binaries, like GW150914;**
- **(iii) could alert laser interferometers days before merger by detecting inspiral phase and predict time of binany black hole coalescence & neutron star coalescence for ground interferometers**
- **(iv) Relic/Inflationary GW Background.**

PHYSICAL REVIEW D **88**, 122003 (2013)

Low-frequency terrestrial gravitational-wave detectors

Jan Harms,[1] Bram J. J. Slagmolen,[2] Rana X. Adhikari,[3] M. Coleman Miller,[4,5] Matthew Evans,[6] Yanbei Chen,[7] Holger Müller,[8] and Masaki Ando[9,10]

Direct detection of gravitational radiation in the audio band is being pursued with a network of kilometer-scale interferometers (LIGO, Virgo, KAGRA). Several space missions (LISA, DECIGO, BBO) have been proposed to search for sub-hertz radiation from massive astrophysical sources. Here we examine the potential sensitivity of three ground-based detector concepts aimed at radiation in the 0.1–10 Hz band. We describe the plethora of potential astrophysical sources in this band and make estimates for their event rates and thereby, the sensitivity requirements for these detectors. The scientific payoff from measuring astrophysical gravitational waves in this frequency band is great. Although we find no fundamental limits to the detector sensitivity in this band, the remaining technical limits will be extremely challenging to overcome.

- **Analyzed three detector options:**
  1. **Atom-laser interferometer**
  2. **TOBA with laser interferometer**
  3. **Michelson interferometer**
- **Would be astrophysically interesting, if one can reach $S_h^{1/2}(f) = 10^{-20}$ Hz$^{-1/2}$ in 0.1-10 Hz band.**
- **Detecting and removing NN appears to be *extremely challenging*.**

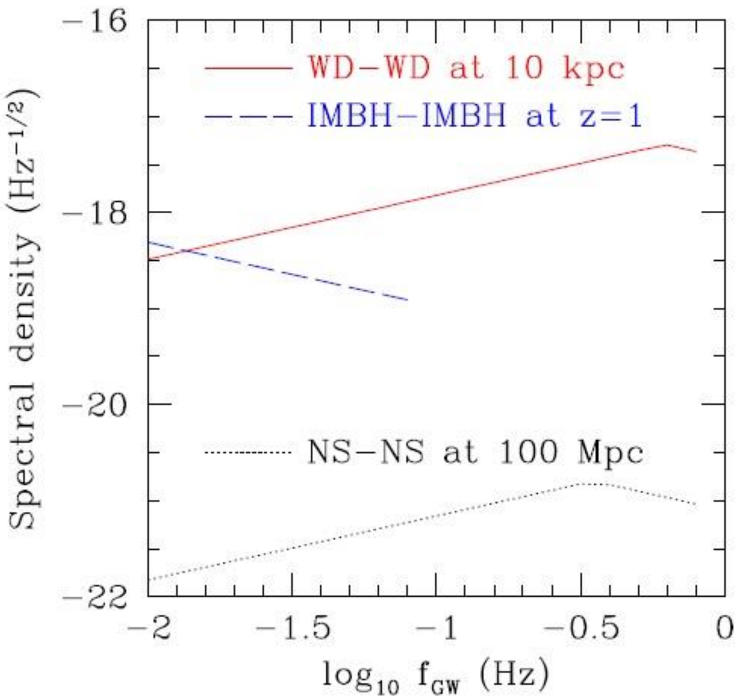

Proposed Detection Methods for Middle-frequency GWs

- TOBA – The torsion bar antenna
- SOBRO -- Superconducting Omni-directional Gravitational Radiation Observatory
- Michelson Interferometer on Earth and in space
- Atom Interferometry involving repeatedly imprinting the phase of optical field onto the motional degrees of freedom of the atoms using light propagating back and forth between the spacecraft.
- Resonant Atom Interferometry detection
- Radio-wave Doppler frequency tracking
- GW detection with optical lattice atomic clocks

Torsion-Bar Antenna for Low-Frequency Gravitational-Wave Observations

Masaki Ando,[1,*] Koji Ishidoshiro,[2,†] Kazuhiro Yamamoto,[3] Kent Yagi,[1] Wataru Kokuyama,[2]
Kimio Tsubono,[2] and Akiteru Takamori[4]

- **TOBA – The torsion bar antenna; PRL2010, PRD2013**
- **10 m x 0.6 m ϕ quartz/Al 5056**
- **10 ton each**
- **Fundamental torsion frequency 30 μHz**

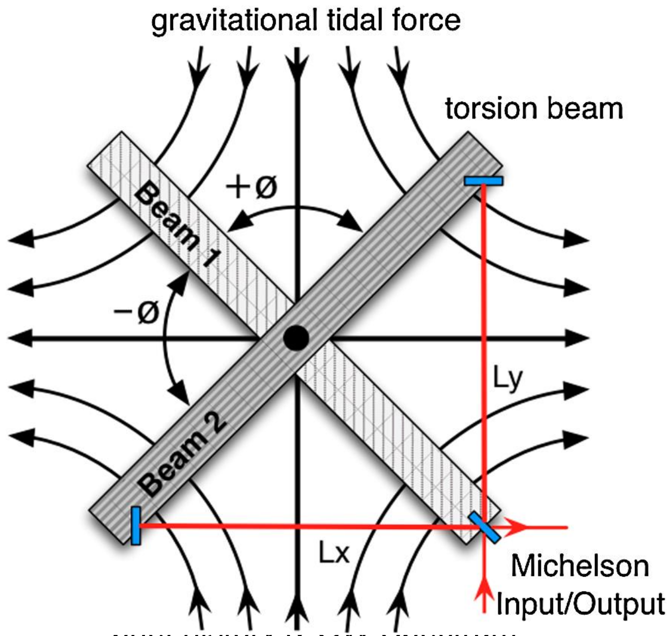

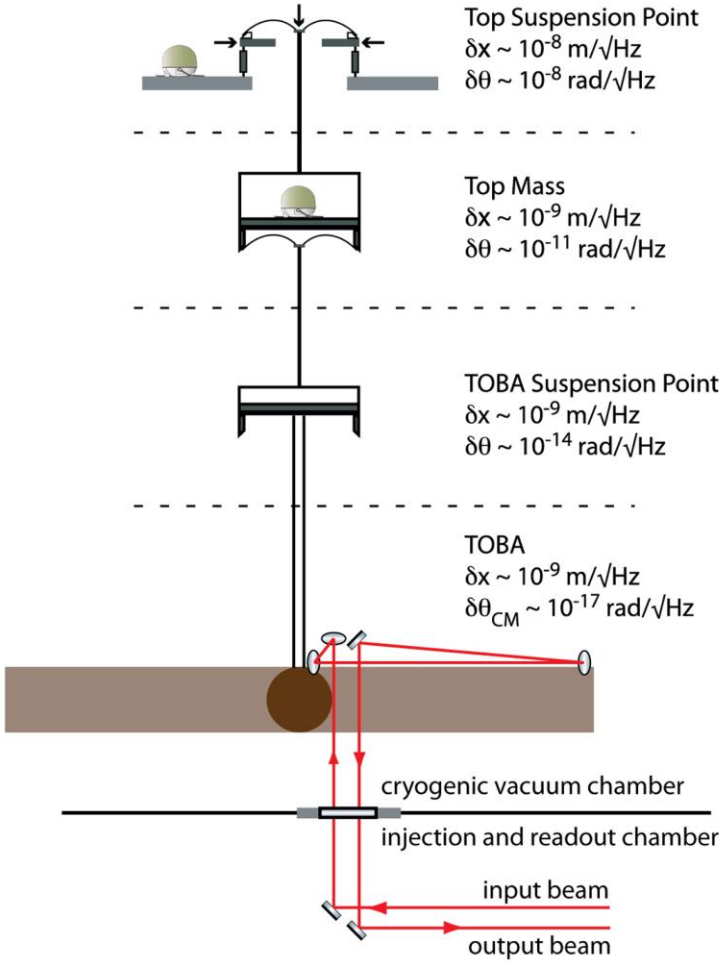

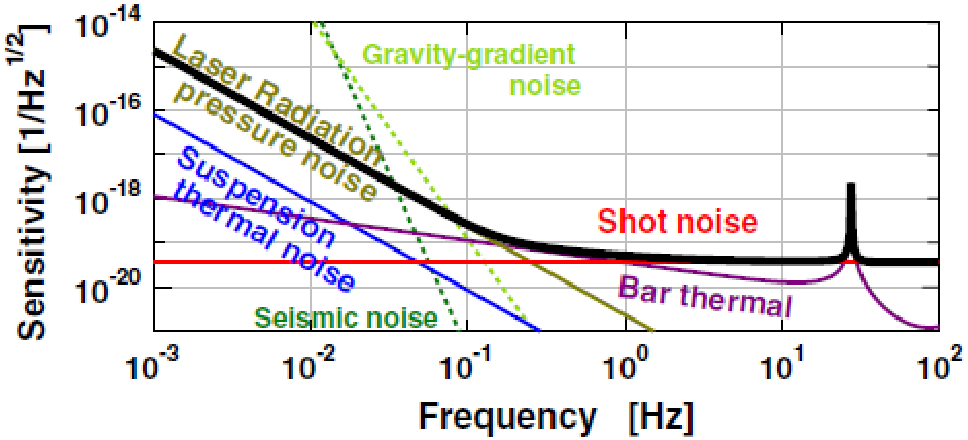

FIG. 2 (color online). Estimated sensitivity of a torsion-bar antenna (thick black curve). Limitations by fundamental noises are shown together.

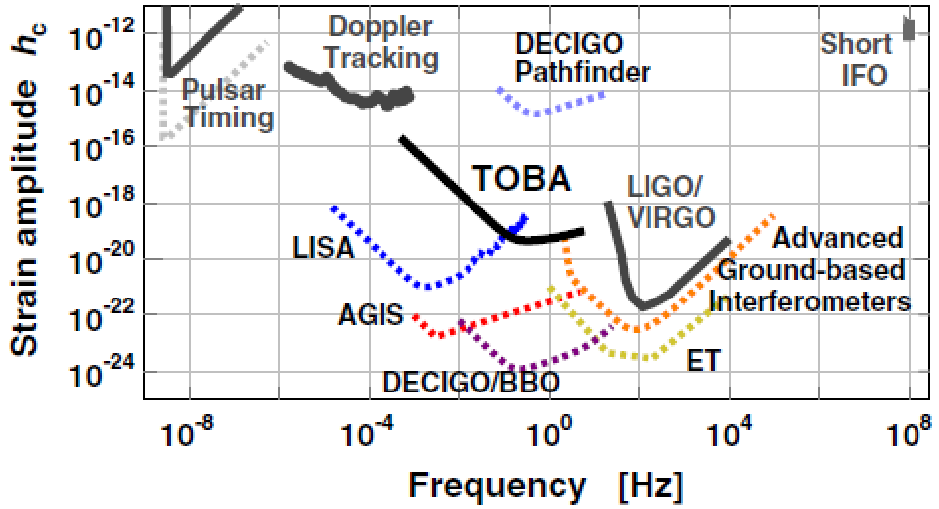

Newtonian Noise – seismic and atmospheric NN would have to be reduced by large factors to achieve sensitivity goals with respect of NN

It is uncertain whether sufficiently sensitive seismic and infrasound sensors can be provided. It will be very challenging to achieve sufficient NN subtraction. A suppression of the NN by about 4 or 5 orders of magnitude at 0.1 Hz would be needed to make it comparable to the instrument noise limit. A larger number of more sensitive sensors will be required.

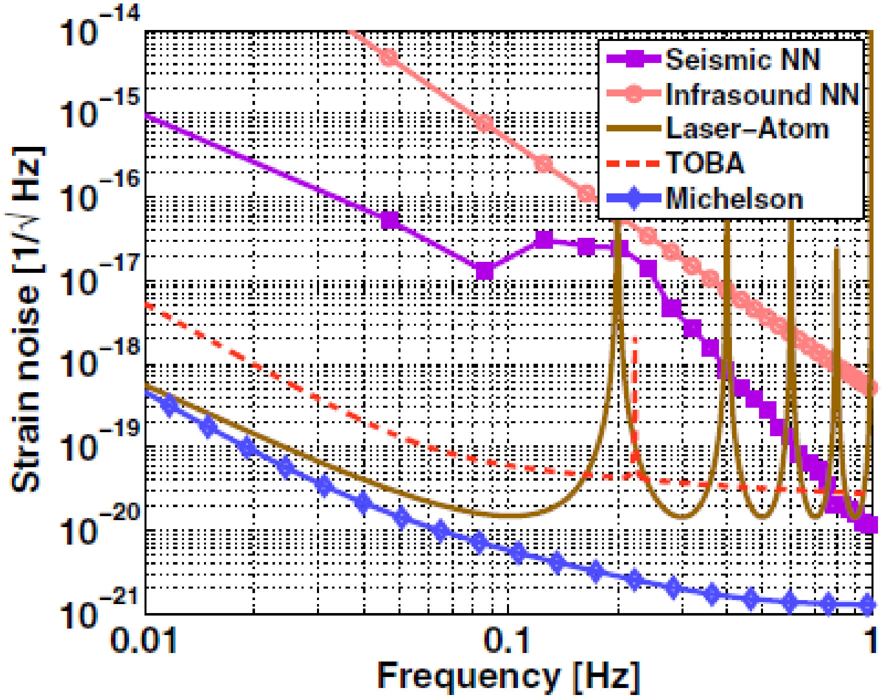

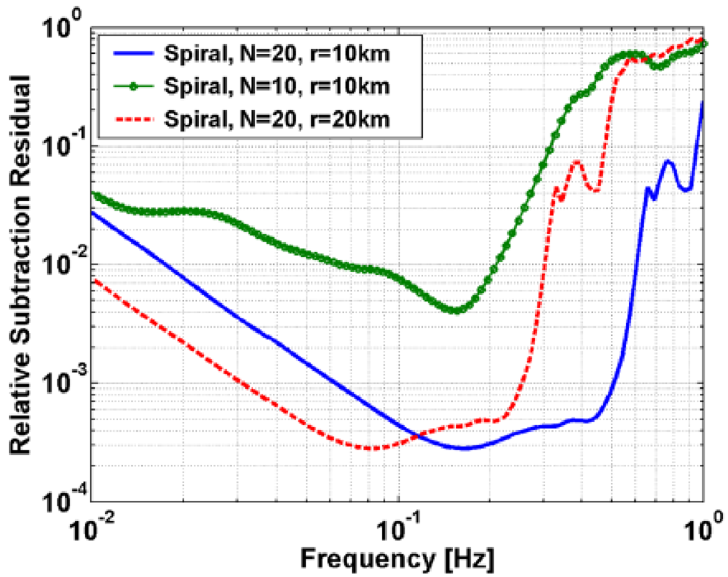

FIG. 10 (color online). Residuals of Rayleigh-wave gradient NN subtraction for double-wound spiral arrays using seismometers with SNR = 1000. Results are presented for different numbers N of seismometers and different array radii r.

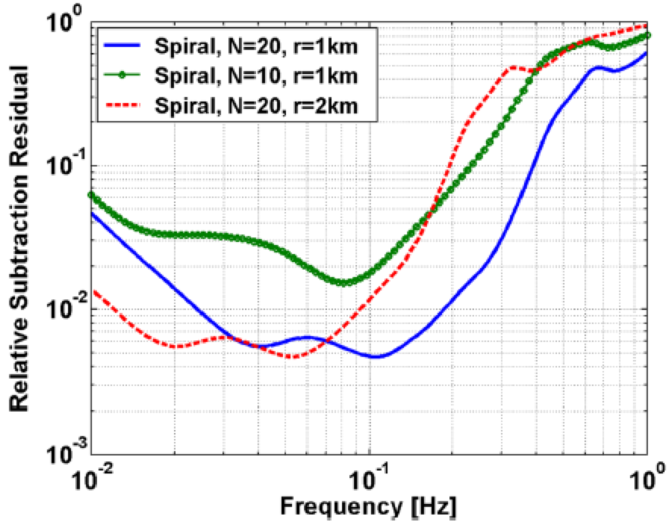

FIG. 11 (color online). Residuals of infrasound gradient NN subtraction for double-wound spiral arrays using microphones with SNR = 1000. Results are presented for different numbers N of microphones and different array radii r.

SOGRO (Paik et al 2016)
(Superconducting Omni-directional Gravitational Radiation Observatory)

A design concept that could reach a strain sensitivity of 10^{-19}–10^{-20} Hz$^{-1/2}$ at 0.2–10 Hz

the range of the WD–WD binary from 0.1 Hz for one year with a SNR of 10 is 1.2 Mpc, assuming one solar mass ($M_\odot$) for the WD mass. Within this horizon, there are two massive galaxies: the Milky Way Galaxy and Andromeda (M31). The WD–WD merger rate of ~1.4×10^{-13} yr^{-1}$M_\odot^{-1}$ has been estimated, corresponding to 0.01 per year for our Galaxy. With M31 about 0.03 per year. Probability of finding a WD–WD binary merger during one-year operation of SOGRO is ~30% since each event is expected to persist for ~10 years in the detector.

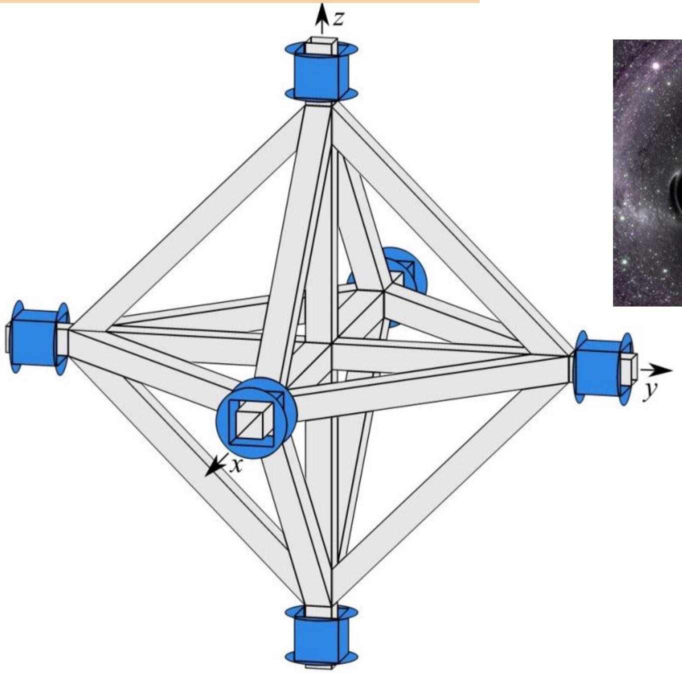

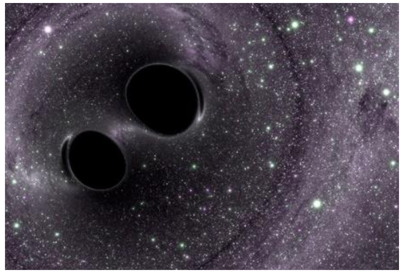

Binary mergers composed of IMBHs can be detected by SOGRO up to several Gpc (see figure 1). The estimated rates of mergers are very uncertain, but up to a few tens of IMBH mergers can be detected per year by SOGRO [7].

Each test mass M	5 ton	Nb square tube
Arm length L	30-50 m	Over a 'rigid' platform
Antenna temperature T	1.5 K	Superfluid helium or cryocoolers
DM quality factor	5×10^8	Surface-polished pure Nb
Signal frequency f	0.1–10 Hz	

Ho Jung Paik

Department of Physics, University of Maryland

ICGAC-XIII, Seoul, July 4, 2017

Space GW Detection Science Goals

- The science goals are the detection of GWs from

- (i) Supermassive Black Holes;
- (ii) Extreme-Mass-Ratio Black Hole Inspirals;
- (iii) Intermediate-Mass Black Holes;
- (iv) Galactic Compact Binaries;
- (v) Detecting inspiral phase and predict time of binary black hole coalescence for ground interferometers
- (vi) Relic/Inflationary GW Background.

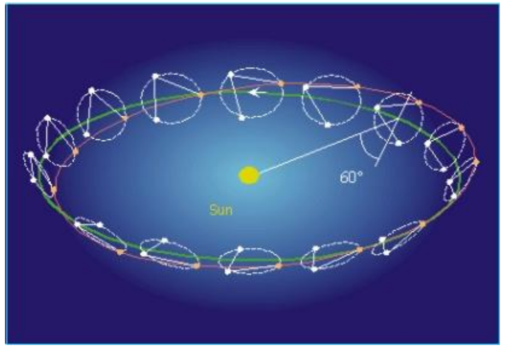

空间引力波探测
A Compilation of GW Mission Proposals LISA Pathfinder Launched on December 3, 2015

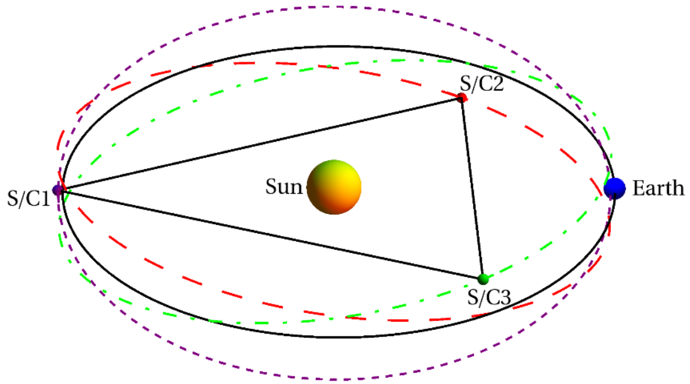

Mission Concept	S/C Configuration	Arm length	Orbit Period	S/C #
Solar-Orbit GW Mission Proposals				
LISA[65]	Earth-like solar orbits with 20° lag	5 Gm	1 year	3
eLISA[64]	Earth-like solar orbits with 10° lag	1 Gm	1 year	3
ASTROD-GW[68]	Near Sun-Earth L3, L4, L5 points	260 Gm	1 year	3
Big Bang Observer[73]	Earth-like solar orbits	0.05 Gm	1 year	12
DECIGO[72]	Earth-like solar orbits	0.001 Gm	1 year	12
ALIA[74]	Earth-like solar orbits	0.5 Gm	1 year	3
ALIA-descope[75] 太极	Earth-like solar orbits	3 Gm	1 year	3
Super-ASTROD[71]	Near Sun-Jupiter L3, L4, L5 points (3 S/C), Jupiter-like solar orbit(s)(1-2 S/C)	1300 Gm	11 year	4 or 5
Earth-Orbit GW Mission Proposals				
OMEGA[81]	0.6 Gm height orbit	1 Gm	53.2 days	6
gLISA/GEOGRAWI[76-78]	Geostationary orbit	0.073 Gm	24 hours	3
GADFLI[79]	Geostationary orbit	0.073 Gm	24 hours	3
TIANQIN[82] 天琴	0.057 Gm height orbit	0.11 Gm	44 hours	3
ASTROD-EM[69,70]	Near Earth-Moon L3, L4, L5 points	0.66 Gm	27.3 days	3
LAGRANGE[80]	Near Earth-Moon L3, L4, L5 points	0.66 Gm	27.3 days	3

Mission concept	S/C configuration	Arm length	Orbit period	S/C #	Acceleration noise [$\mathrm{fm/s^2/Hz^{1/2}}$]	Laser metrology noise [$\mathrm{pm/Hz^{1/2}}$]
			Solar-Orbit GW Mission Proposals			
LISA[9]	Earthlike solar orbits with 20° lag	5 Gm	1 year	3	3	20
eLISA[21]	Earthlike solar orbits with 10° lag	1 Gm	1 year	3	3	12(10)
ASTROD-GW[36–40]	Near Sun–Earth L3, L4, L5 points	260 Gm	1 year	3	3	1000
Big Bang Observer[45]	Earthlike solar orbits	0.05 Gm	1 year	12	0.03	1.4×10^{-5}
DECIGO[44]	Earthlike solar orbits	0.001 Gm	1 year	12	0.0004	2×10^{-6}
ALIA[47]	Earthlike solar orbits	0.5 Gm	1 year	3	0.3	0.6
TAIJI (ALIA-descope)[48]	Earthlike solar orbits	3 Gm	1 year	3	3	5–8
Super-ASTROD[42]	Near Sun–Jupiter L3, L4, L5 points (3 S/C), Jupiterlike solar orbit(s)(1–2 S/C)	1300 Gm	11 year	4 or 5	3	5000
			Earth-Orbit GW Mission Proposals			
OMEGA[54,55]	0.6 Gm height orbit	1 Gm	53.2 days	6	3	5
gLISA/GEOGRAWI[49–51]	Geostationary orbit	0.073 Gm	24 h	3	3, 30	0.3, 10
GADFLI[52]	Geostationary orbit	0.073 Gm	24 h	3	0.3, 3, 30	1
TIANQIN[19]	0.057 Gm height orbit	0.11 Gm	44 h	3	1	1
ASTROD-EM[43]	Near Earth–Moon L3, L4, L5 points	0.66 Gm	27.3 days	3	1	1
LAGRANGE[53]	Earth–Moon L3, L4, L5 points	0.66 Gm	27.3 days	3	3	5

Strain power spectral density (psd) amplitude vs. frequency for various GW detectors and GW sources. [CSDT: Cassini Spacecraft Doppler Tracking; SMBH-GWB: Supermassive Black Hole-GW Background.]

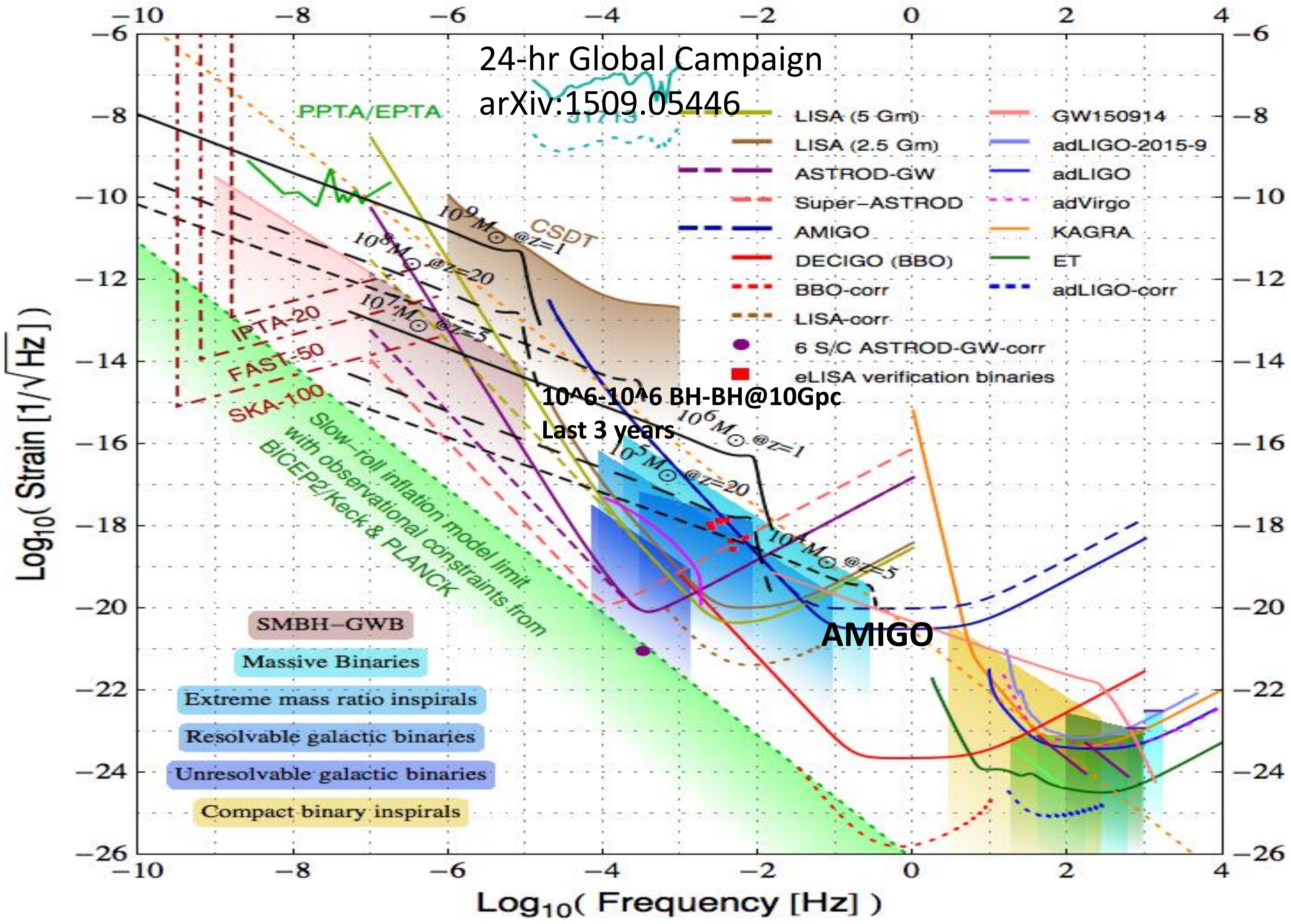

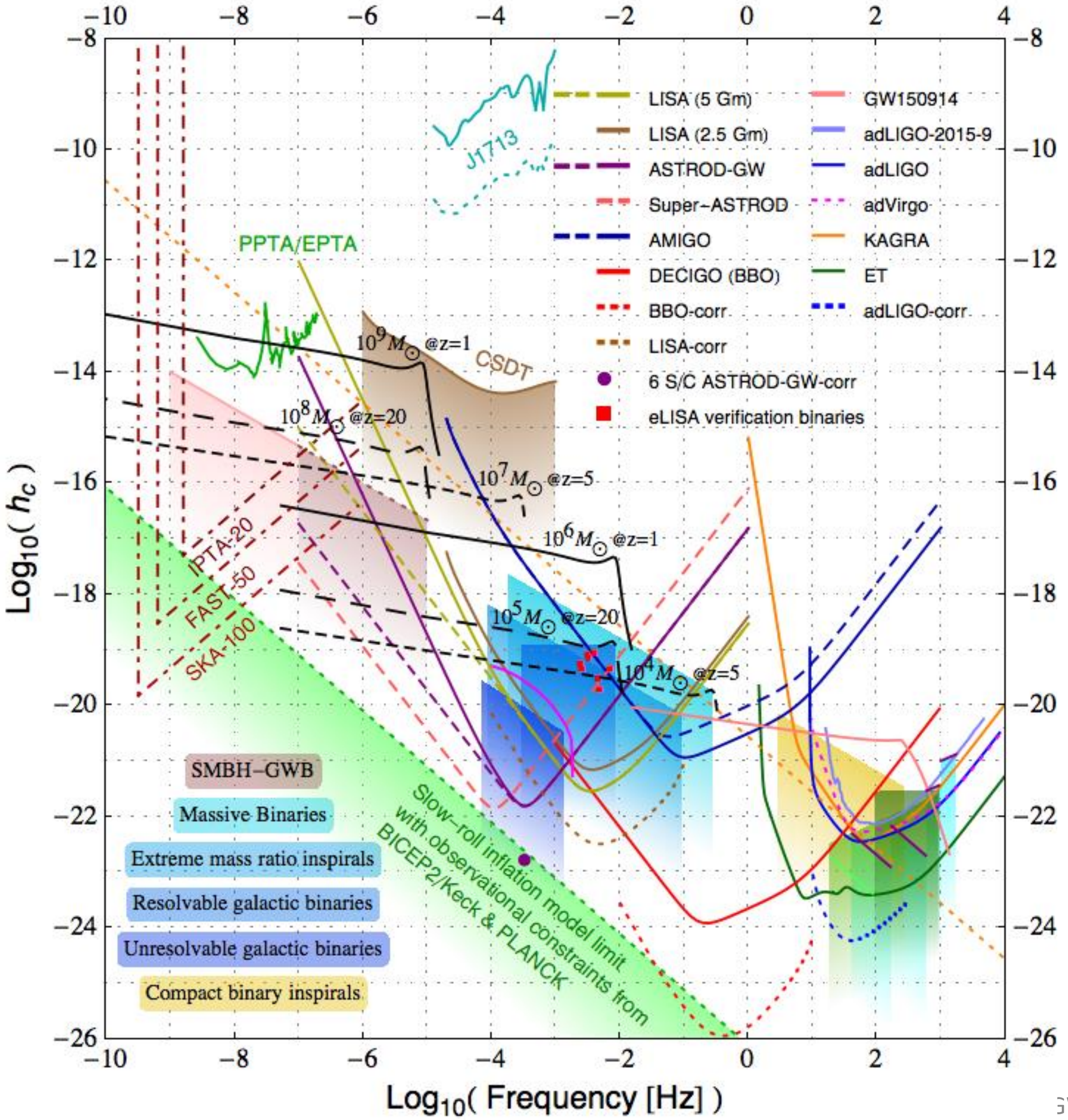

LISA (5 Gm)
LISA (2.5 Gm)
ASTROD-GW
Super-ASTROD
AMIGO
DECIGO (BBO)
BBO-corr
LISA-corr
6 S/C ASTROD-GW-corr
eLISA verification binaries
GW150914
adLIGO-2015-9
adLIGO
adVirgo
KAGRA
ET
adLIGO-corr
J1713
PPTA/EPTA
CSDT
IPTA-20
FAST-50
SKA-100
SMBH−GWB
Massive Binaries
Extreme mass ratio inspirals
Resolvable galactic binaries
Unresolvable galactic binaries
Compact binary inspirals
Slow−roll inflation model limit with observational constraints from BICEP2/Keck & PLANCK
$\mathrm{Log}_{10}(h_c)$
Log_{10}(Frequency [Hz])

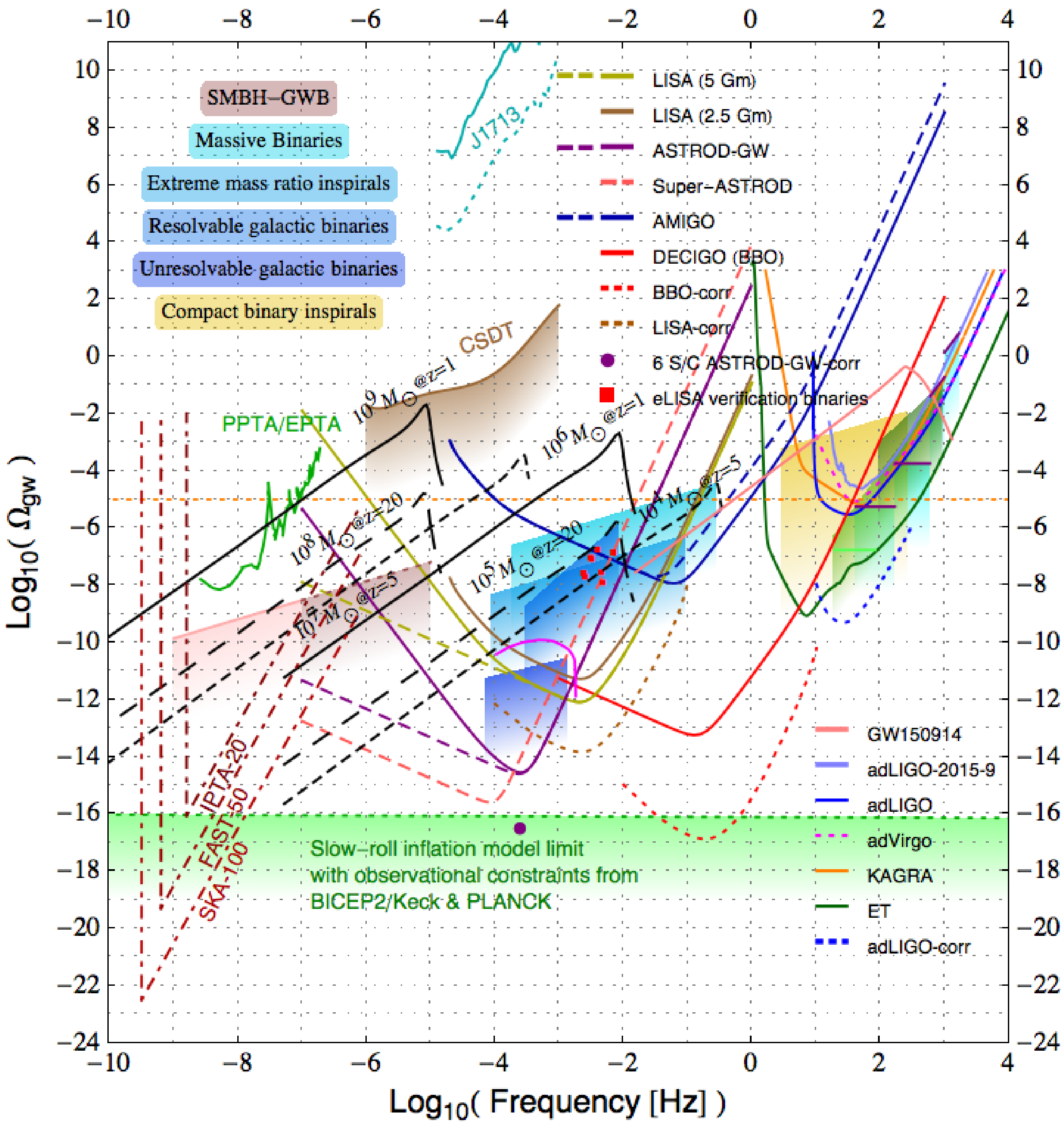

SMBH−GWB
Massive Binaries
Extreme mass ratio inspirals
Resolvable galactic binaries
Unresolvable galactic binaries
Compact binary inspirals
LISA (5 Gm)
LISA (2.5 Gm)
ASTROD-GW
Super-ASTROD
AMIGO
DECIGO (BBO)
BBO-corr
LISA-corr
6 S/C ASTROD-GW-corr
eLISA verification binaries
GW150914
adLIGO-2015-9
adLIGO
adVirgo
KAGRA
ET
adLIGO-corr
J1713
PPTA/EPTA
CSDT
IPTA-20
FAST-50
SKA-100
Slow−roll inflation model limit with observational constraints from BICEP2/Keck & PLANCK
$\mathrm{Log}_{10}(\Omega_{gw})$
Log_{10}(Frequency [Hz])

Second Generation GW Mission Concepts

- DECIGO
- BBO
- Super-ASTROD

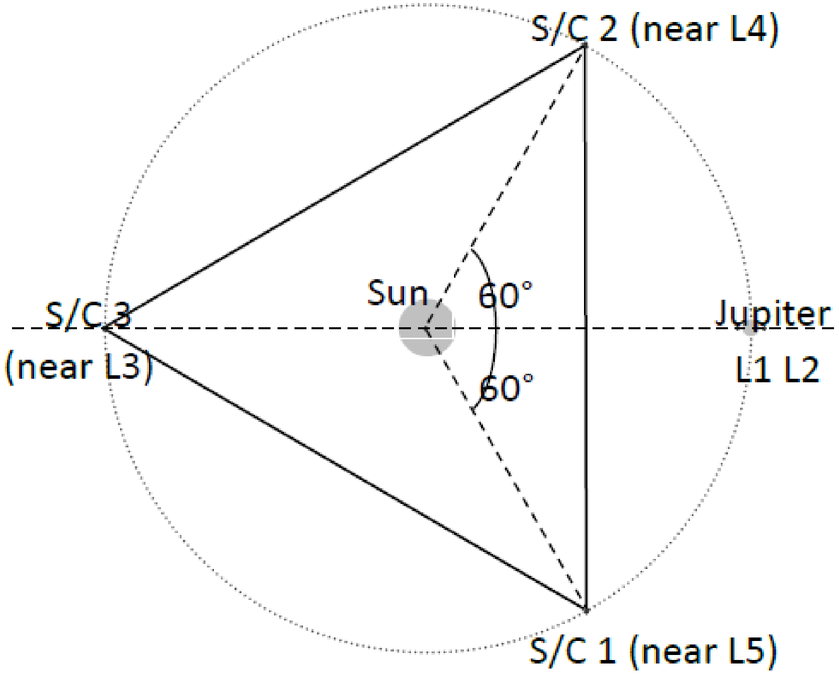

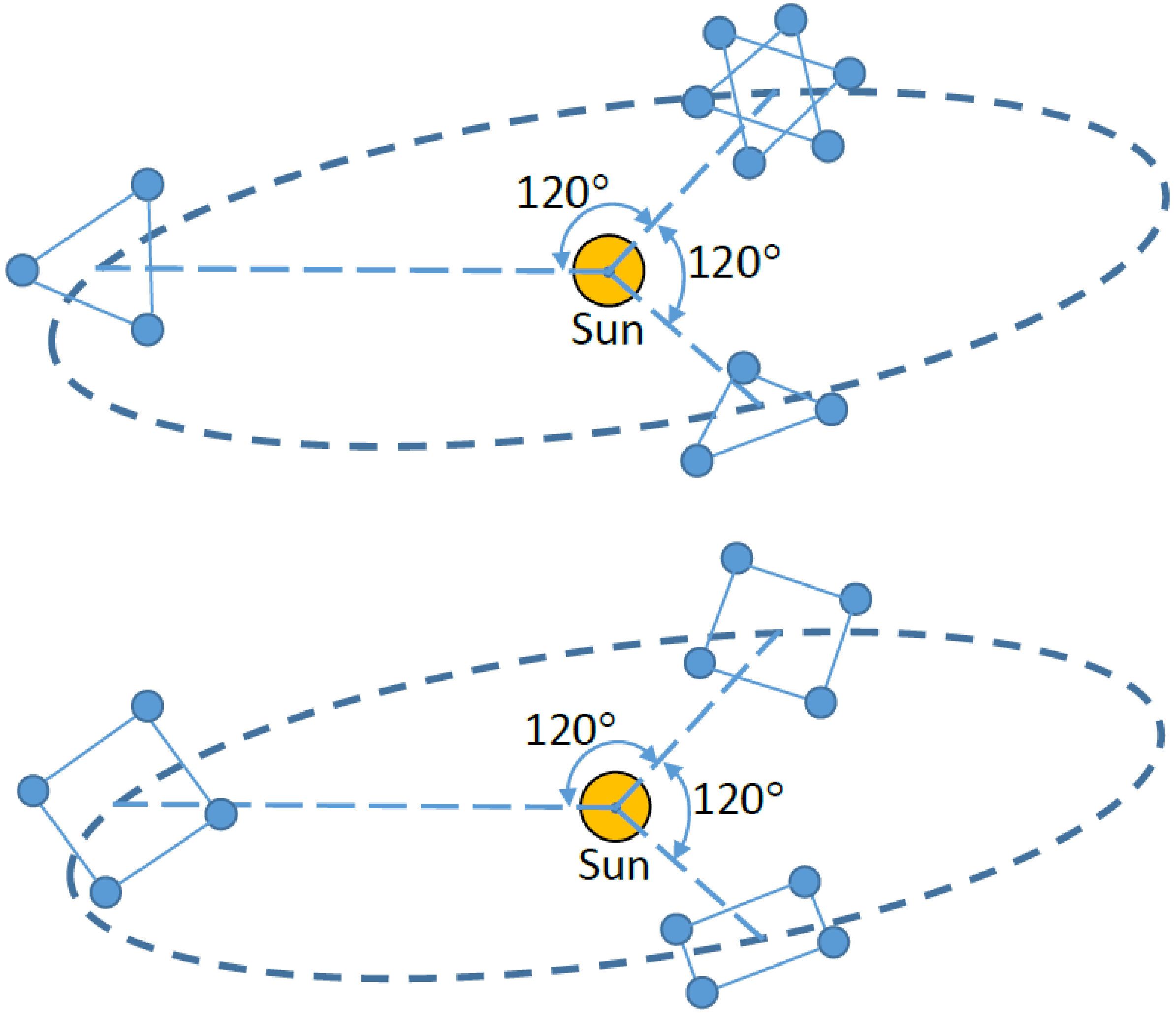

10^(-15) Source-Observation Gap largely bridged

92 days
1440 orbits
83.60 kg mass

- In 1915, white dwarf already discovered, the technology reached 10^(-5). First artificial satellite Sputnik launched in 1957.
- First GW space mission proposed in public in 1981 by Faller & Bender
- LISA proposed as a joint ESA-NASA mission; LISA Pathfinder successfully performed. The drag-free tech is fully demonstrated paving the road for GW space missions.

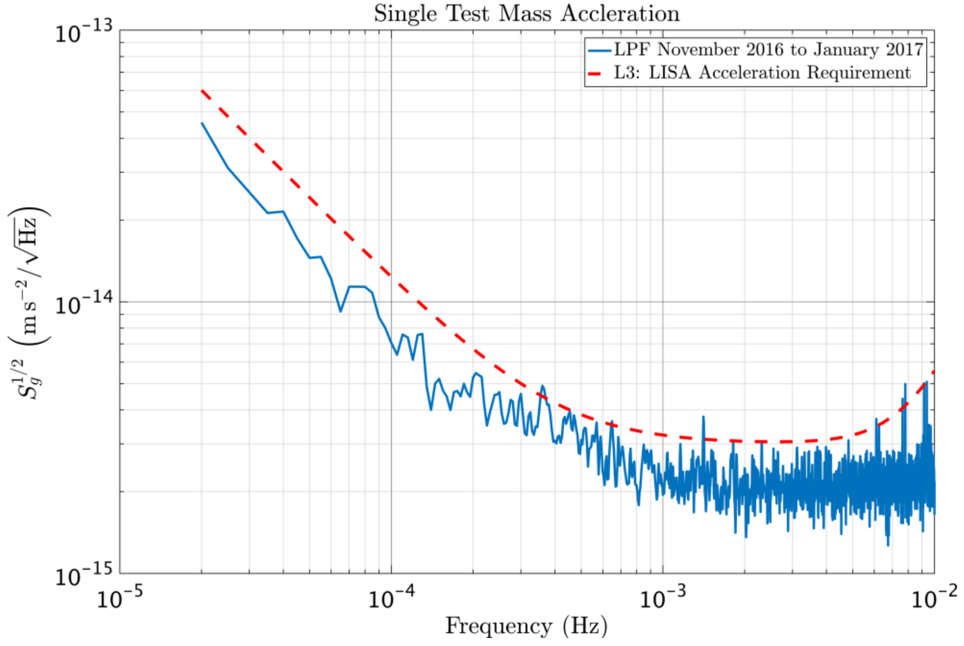

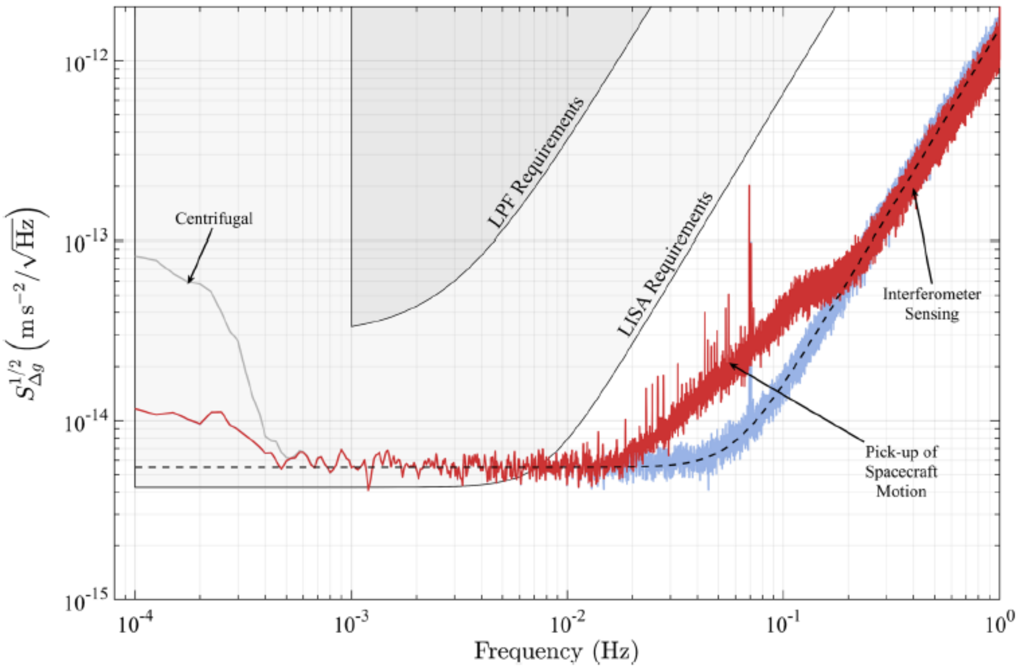

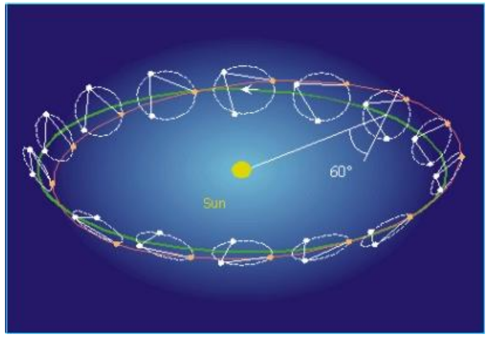

Weak-light phase locking and manipulation technology

- Weak-light phase locking is crucial for long-distance space interferometry and for CW laser space communication. For LISA of arm length of 5 Gm (million km) the weak-light phase locking requirement is for 70 pW laser light to phase-lock with an onboard laser oscillator. For ASTROD-GW arm length of 260 Gm (1.73 AU) the weak-light phase locking requirement is for 100 fW laser light to lock with an onboard laser oscillator.
- Weak-light phase locking for 2 pW laser light to 200 μW local oscillator is demonstrated in our laboratory in Tsing Hua U.[6]
- Dick *et al.*[7] from their phase-locking experiment showed a PLL (Phase Locked Loop) phase-slip rate below one cycle slip per second at powers as low as 40 femtowatts (fW).
- Shaddock et al: tracking 30 fW free-running laser (2015-2016)

The present laser stability (16 orders) alone does not meet the GW strain sensitivity requirement (21 orders)

- For space laser-interferometric GW antenna, the arm lengths vary according to solar system orbit dynamics.
- In order to attain the requisite sensitivity, laser frequency noise must be suppressed below the secondary noises such as the optical path noise, acceleration noise etc.
- For suppressing laser frequency noise, it is necessary to use TDI in the analysis to match the optical path length of different beam paths closely.
- The better match of the optical path lengths is, the better cancellation of the laser frequency noise and the easier to achieve the requisite sensitivity. In case of exact match, the laser frequency noise is fully canceled, as in the original Michelson interferometer.

AMIGO: **A**strodynamical **M**iddle-frequency **I**nterferometric **GW** **O**bservatory

- Arm length: 10,000 km (or a few times)
- Laser power: 2-10 W (or more)
- Acceleration noise: assuming LPF noise
- Orbit: 4 options (all LISA-like formations):

  (i) Earth-like solar orbit (3-20 degrees behind the Earth orbit)

  (ii) 600,000 km high orbits around the

  (iii) 100,000 km-250,000 high orbits around the Earth

  (iv) near Earth-Moon L4 and L5 orbits
- Scientific Goal: to bridge the gap between high-frequency and low-frequency GW sensitivities. Detecting intermediate mass BH coalescence. Detecting inspiral phase and predict time of binary black hole coalescence together with neutron star coalescence for ground interferometers, detecting compact binary inspirals for studying stellar evolution and galactic poulation

GW Sensitivities of AMIGO

- Baseline Sensitivity: 2 W emitting laser power, 300 mm ϕ telescope
- $S_{\mathrm{AMIGOn}}{}^{1/2}(f)=(20/3)^{1/2}(1/L_{\mathrm{AMIGO}})\times[(1+(f/(1.29f_{\mathrm{AMIGO}}))^2)]^{1/2}\times[(S_{\mathrm{AMIGOp}}+4S_a/(2\pi f)^4)]^{1/2}\mathrm{Hz}^{-1/2}$,
- over the frequency range of 20 μHz < f < 1 kHz. Here $L_{\mathrm{AMIGO}} = 0.01 \times 10^9$ m is the AMIGO arm length, $f_{\mathrm{AMIGO}} = c/(2\pi L_{\mathrm{AMIGO}})$ is the AMIGO arm transfer frequency, $S_{\mathrm{AMIGOp}} = 1.424 \times 10^{-28}$ m^2 Hz^{-1} is the (white) position noise level due to laser shot noise which is 16×10^{-6} ($=0.004^2$) times that for new LISA. $S_a(f)$ is the same colored acceleration noise level in (2)
- Design Sensitivity: 10 W emitting laser power, 360 mm ϕ telescope

Shot noise for strain to gain a factor of

10 [≈ (10W/2W)×(360mm/300mm)^4]

AMIGO solid curve by using $S_{\mathrm{AMIGOp}} = 0.1424 \times 10^{-28}$ m^2 Hz^{-1}.

LISA 2.5 Gm Sensitivity

- The new LISA design sensitivity is in [10, 11]. A simple analytical approximation of the design sensitivity is in Petiteau et al. [10] and used by Cornish and Robson [26]:

- $S_{\mathrm{Ln}}{}^{1/2}(f) = (20/3)^{1/2}\,(1/L_{\mathrm{L}}) \times [(1 + (f\,/\,(1.29 f_{\mathrm{L}}))^2\,)]^{1/2} \times [(S_{\mathrm{Lp}} + 4S_{\mathrm{a}}/(2\pi f)^4)]^{1/2}\ \mathrm{Hz}^{-1/2},$ (1)
- over the frequency range 20 μHz $< f <$ 1 Hz. Here L_{L} = 2.5 Gm is the LISA arm length, $f_{\mathrm{L}} = c\,/\,(2\pi L_{\mathrm{L}})$ is the LISA arm transfer frequency, $S_{\mathrm{Lp}} = 8.9 \times 10^{-23}\ \mathrm{m}^2\ \mathrm{Hz}^{-1}$ is the white position noise, and

- $S_{\mathrm{a}}(f) = 9 \times 10^{-30}\ \ [1 + (10^{-4}\ \mathrm{Hz}/\,f\,)^2 + 16\,(2 \times 10^{-5}\ \mathrm{Hz}/\,f\,)^{10}\,]\ \mathrm{m}^2\ \mathrm{s}^{-4}\ \mathrm{Hz}^{-1},$ (2)

- is the colored acceleration noise level. This new LISA design sensitivity curve shows in both Fig. 1 and Fig. 2.

Orbit design: Earth-like solar orbits

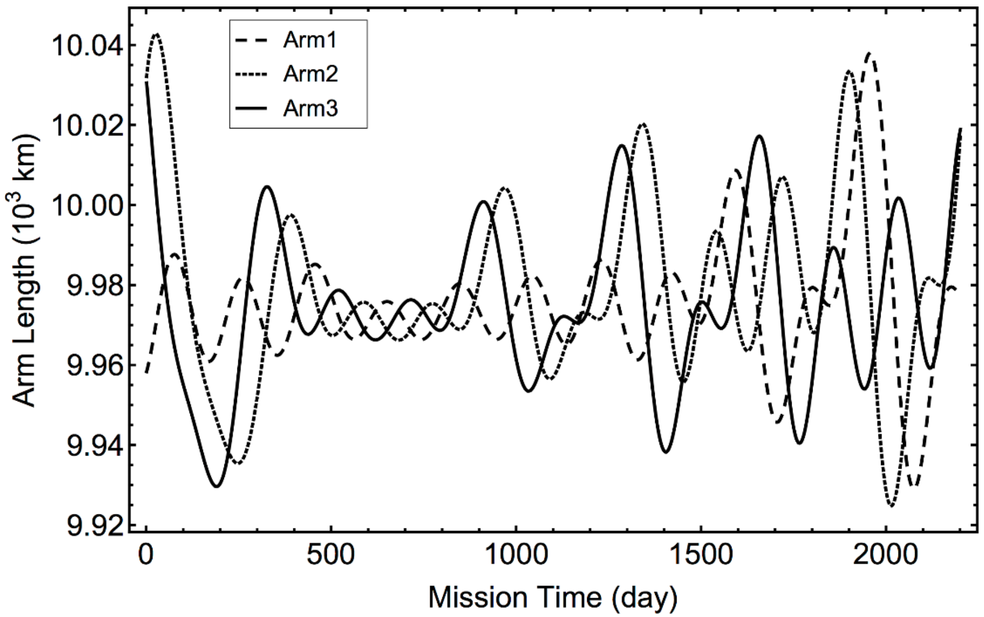

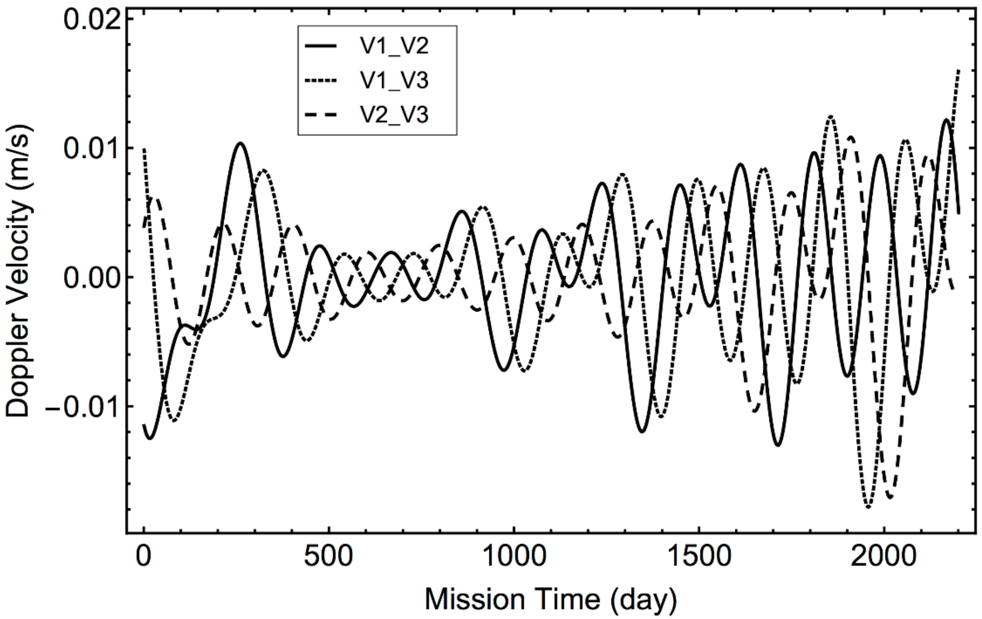

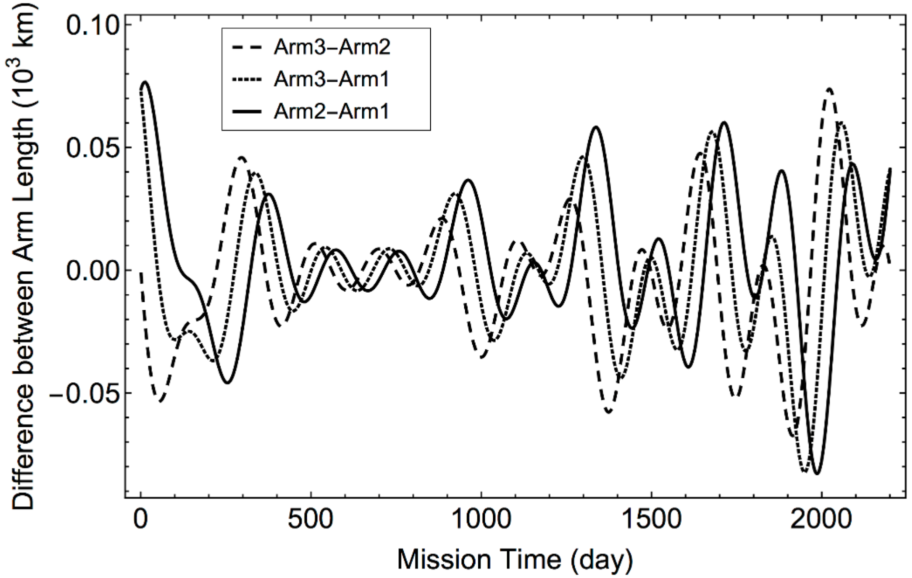

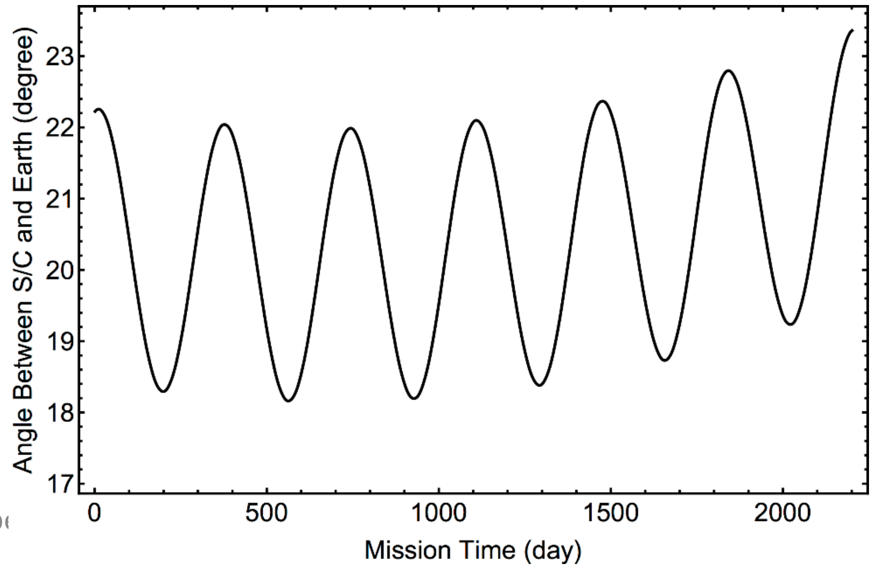

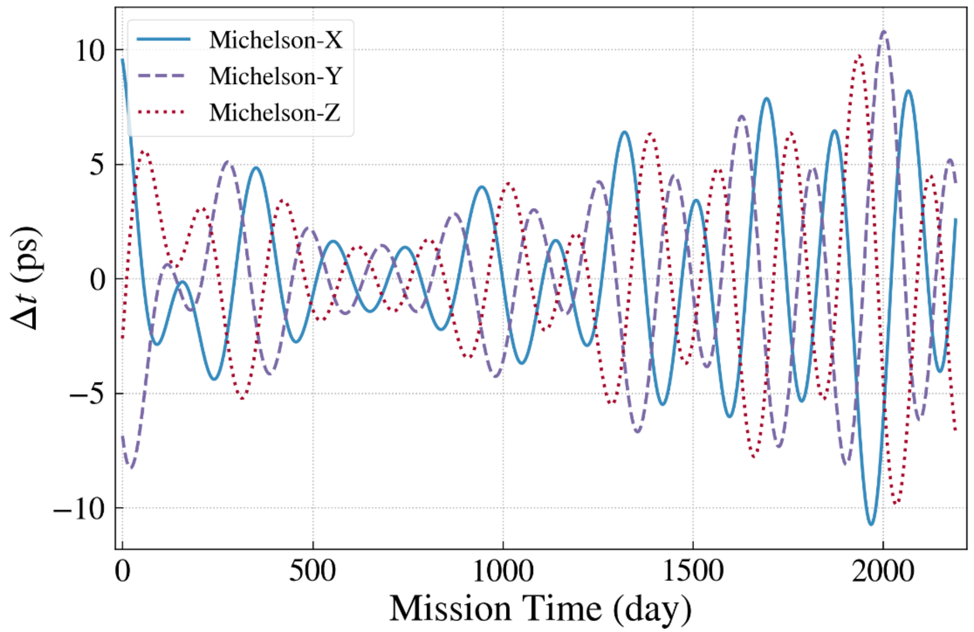
Michelson-X
Michelson-Y
Michelson-Z
Δt (ps)
Mission Time (day)

T
D
I

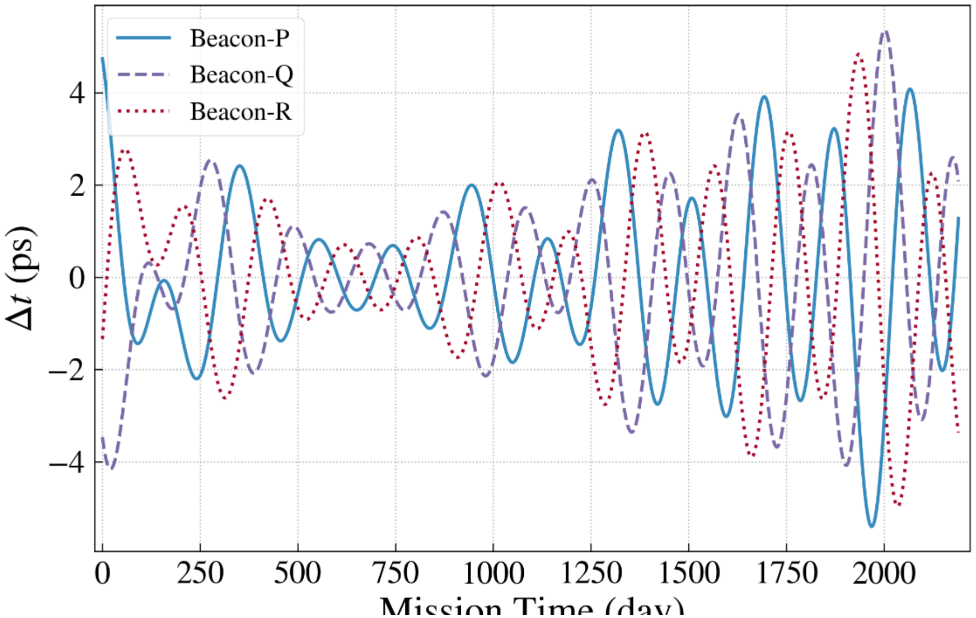
Beacon-P
Beacon-Q
Beacon-R
Δt (ps)
Mission Time (day)

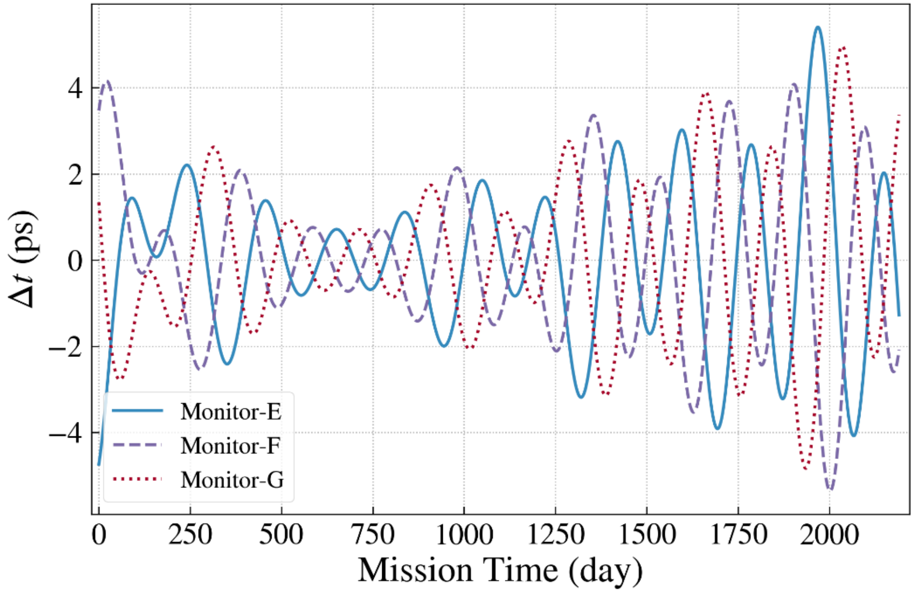
Monitor-E
Monitor-F
Monitor-G
Δt (ps)
Mission Time (day)

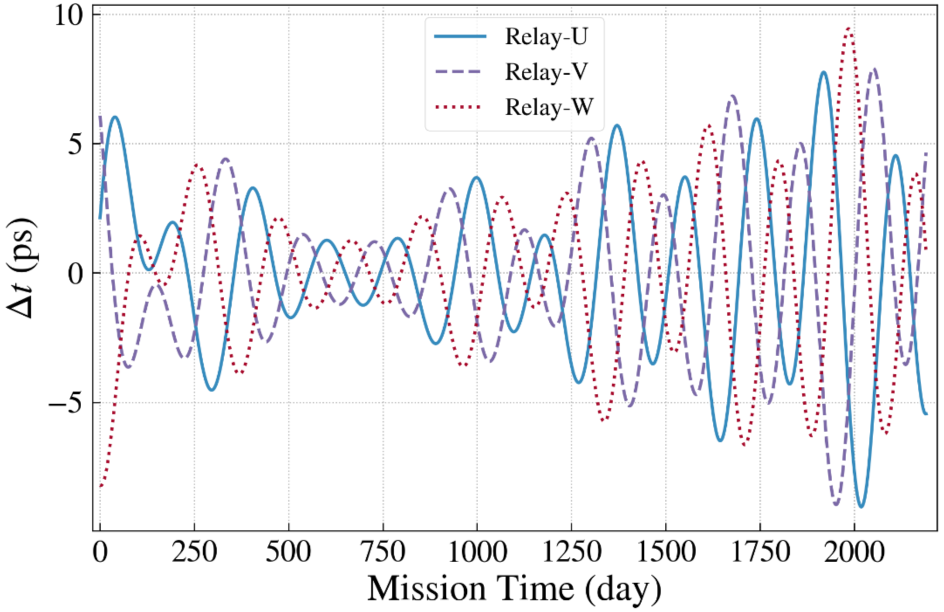
Relay-U
Relay-V
Relay-W
Δt (ps)
Mission Time (day)

Time Delay Interferometry

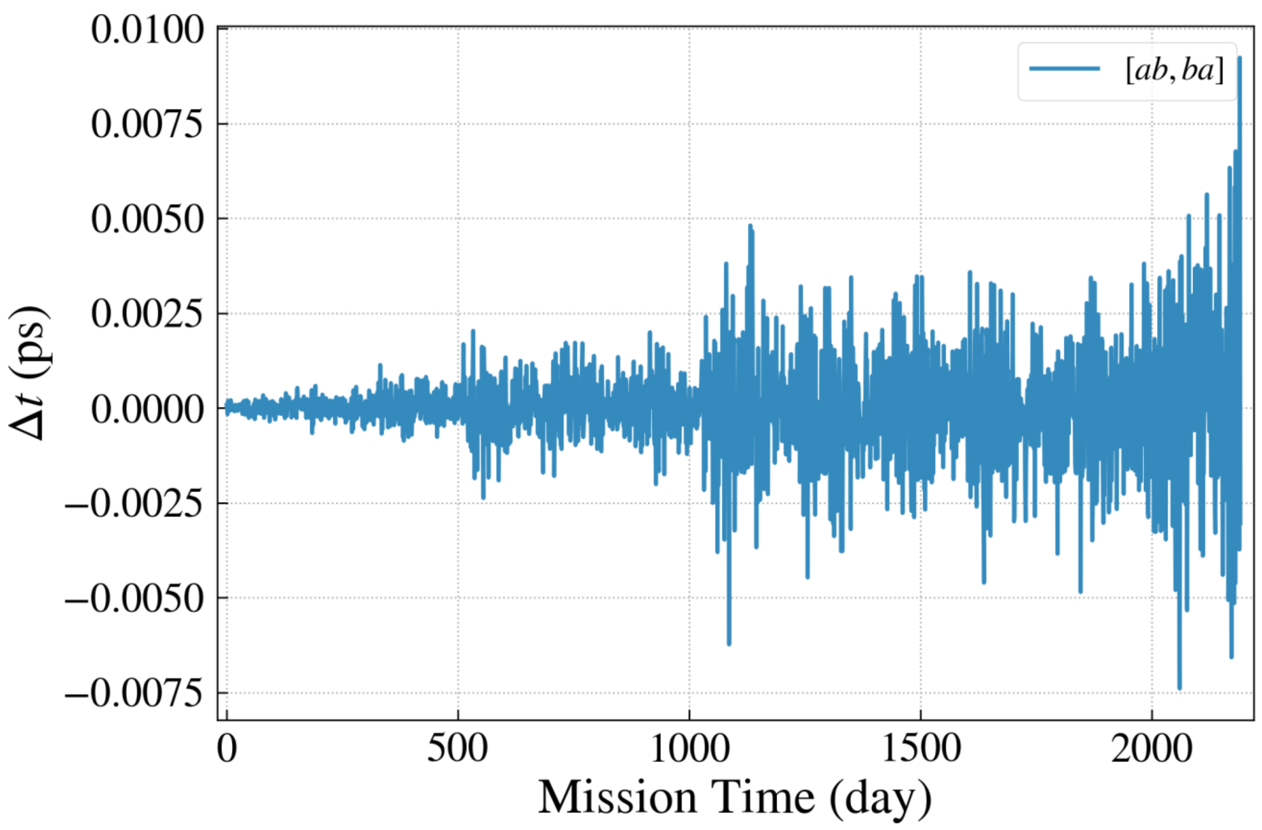

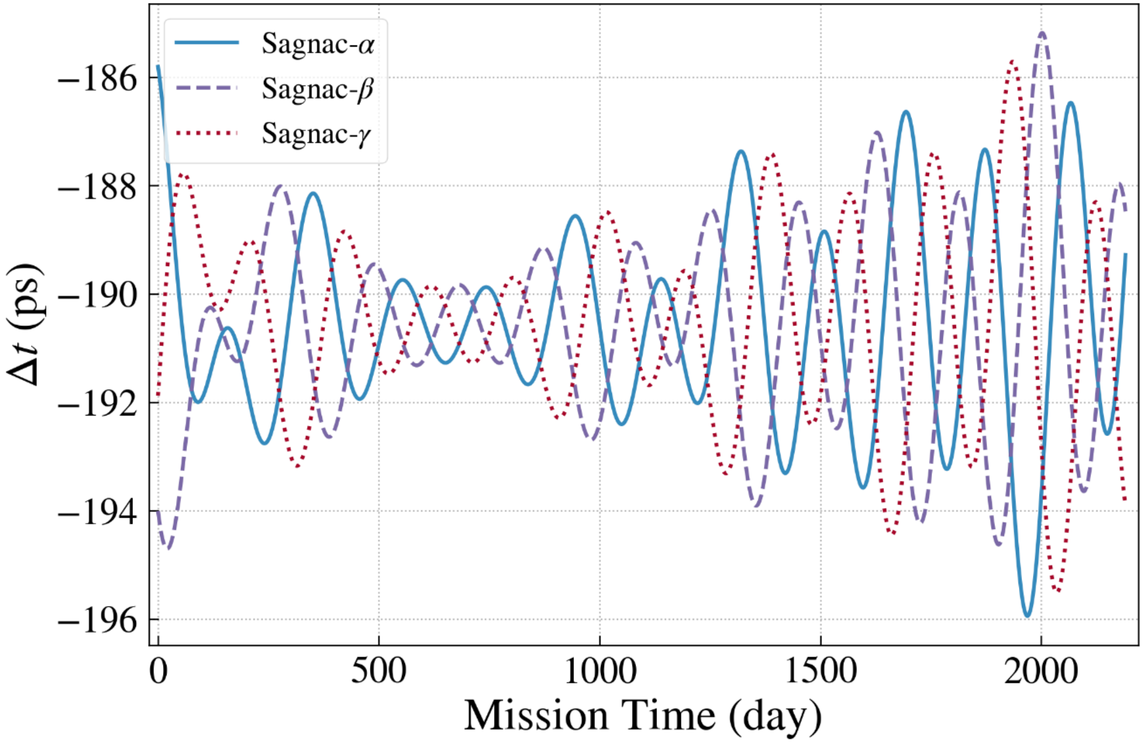

Space Detection Methods other than Laser Interferometry for Low-frequency and Middle-frequency GWs

- Radio-wave Doppler frequency tracking
- Atom Interferometry involving repeatedly imprinting the phase of optical field onto the motional degrees of freedom of the atoms using light propagating back and forth between the spacecraft.
- Resonant Atom Interferometry detection
- GW detection with optical lattice atomic clocks

Summary

- Success of Interferometric Detection of GW
- Stellar-size BH distribution is largely set by observation
- Multi-Messenger Astronomy is started bright
- GW spectrum and detection sensitivities are presented
- Cosmic Band, Quaser Astrometry Band and PTA band
- Space GW detection, new LISA and Super-ASTROD and AMIGO, Middle-Frequency Band
- GW and Multi-Messenger Astronomy: Focus of Next 50 yrs


Thank you